UNIVERSITY OF CALIFORNIA

Santa Barbara

Improvement of DNA-based and protein-based electrochemical biosensors

A Dissertation submitted in partial satisfaction of the

requirements for the degree Doctor of Philosophy

in Chemistry

by

Di Kang

Committee in charge:

Professor Kevin W. Plaxco, Chair

Professor Jacob N. Israelachvili

Professor J. Herbert Waite

Professor R. Daniel Little

September 2016

The dissertation of Di Kang is approved.

_____

Jacob N. Israelachvili

_____

J. Herbert Waite

_____

R. Daniel Little

_____

Kevin W. Plaxco, Committee Chair

August 2016

Improvement of DNA-based and Protein-based Electrochemical Biosensors

by

Di Kang

ACKNOWLEDGMENTS

During these many years, my research project has been supported by many people. I would first like to thank my supervisor, Dr. Kevin Plaxco. He has supported and guided me throughout my entire graduate studies. I am lucky to have had the chance to study and research abroad, and I am very glad that I had the opportunity to join his research group and complete my doctoral studies at UCSB. During my time at UCSB, his broad knowledge has benefited my learning, his sharp scientific sense has guided my research, and his kind and generous personality has touched my life. I appreciate that he gives me absolute freedom and trust in my research, and always encourages and helps me when I face difficulty.

I would like to thank my dissertation committee, Dr. Jacob Israelachvili, Dr. Herbert Waite and Dr. Daniel Little, who were supportive and dedicated to my research and Dr. Frederick Dahlquist for his support and collaboration.

Research needs teamwork. Without the help of my excellent colleagues and knowledgeable collaborators, my research would not have been as rewarding. I give special thanks to the many former and present Plaxco group members, from whom I have learned, and with whom I have shared: Ryan White, Francesco Ricci, Takanori Uzawa, Alexis Vallee-Belisle, Fan Xia, Xiaolei Zhuo, Andrew Bonham, Emir Yasun, Martin Kurnik, Hui Li, Netzahualcóyotl Arroyo, Philippe Ducharme, Claudio Parolo, Gabriel Ortega, Arica Lubin, Kevin Cash, Camille Lawrence, Adriana Patterson, Aaron Rowe, Herschel Watkins, Hannah Kallewaard-Lum, Anna Simon, Jacob Somerson, Megan Larisch and Ava Shruti Greenwood. I give very special thanks to Ryan White, whose knowledge and patience taught and guided me when I first joined the group, and Francesco Ricci, Alexis Vallée-Bélisle, Fan Xia, Martin Kurnik, who supported and helped me on my later projects. During my research

career at UCSB, I also had opportunities to collaborate with other groups, learning from them a range of different knowledge building good friendships. In organic synthesis these collaborators and friends include Renqiang Yang, Wei Zhong, Wenju Bai. During the collaboration with Sheng Sun, I learned protein chemistry. In surface science I learned from Hongbo Zeng and Jing Yu, and in nanopartical chemistry I learned from Xiao Huang and Dean Morales. All these experiences improved my research both now and in the future. I must also acknowledge our research and administrative support staff, especially including James Pavlovich, Ericka James and Cabe Fletcher.

Finally, I would like to thank all my friends, my wife, and my family. My family has supported me throughout my years of study. My parents have given me financial and spiritual support. They were always standing behind me, growing my courage and consulting on my research. My wife, Chuanfei, whose love always brings me joy, has always encouraged me never to give up during these years. My friends, I have enjoyed so much of my life with them, we discuss science, enjoy food, celebrate festivals, exercise sport together. I would like to thank in particular, Gloria Mo, Macro Lam, Xiqing Wang, Yuan Zhang, and Huiqiong Zhou.

VITA OF DI KANG

August 2016

EDUCATION

Doctor of Philosophy in Chemistry, Department of Chemistry and Biochemistry, University of California Santa Barbara, United States of America, September 2016 (expected)

Master of Science & Technology in Micro & Nano Technology, Department of Information System and Technology, Paris XI University, France, December 2008

Bachelor of Science in Electronic Science And Technology, Department of Material Science and Engineering, Fudan University, China, July 2005

RESEARCH

2010-present	Graduate Researcher, UC. Santa Barbara, USA.
2008-2010	Jr. Specialist, UC. Santa Barbara, USA.
2007-2008	Master's Researcher, Paris XI University, France
2004-2005	Undergraduate Researcher, Fudan University, China

PROFESSIONAL EMPLOYMENT

2005-2006 Product Development Engineer, INTEL Corp. China

PUBLICATIONS

(1) Di Kang, Xiaolei Zuo, Renqiang Yang, Fan Xia, Kevin W. Plaxco and Ryan J. White. "Comparing the Properties of Electrochemical-Based DNA Sensors Employing Different Redox Tags". Analytical Chemistry. 2009, **81** (21), 9109–9113.

(2) Fan Xia, Xiaolei Zuo, Renqiang Yang, Yi Xiao, Di Kang, Alexis Valle-Blisle, Xiong Gong, Alan J. Heeger and Kevin W. Plaxco. "On the Binding of Cationic, Water-Soluble Conjugated Polymers to DNA: Electrostatic and Hydrophobic Interactions". J. Am. Chem. Soc. 2010, **132**, 1252–1254

(3) Fan Xia, Xiaolei Zuo, Renqiang Yang, Yi Xiao, Di Kang, Alexis Vallée-Bélisle, Xiong Gong, Jonathan D. Yuen, Ben B. Y. Hsu, Alan J. Heeger, and Kevin W. Plaxco, "Colorimetric detection of DNA, small molecules, proteins, and ions using unmodified gold nanoparticles and conjugated polyelectrolytes". P. Natl. Acad. Sci. 2010. **107**, 10837-10841

(4) Fan Xia, Ryan White, Xiaolei Zuo, Adriana Patterson, Yi Xiao, Di Kang, Xiong Gong, Alan J. Heeger and Kevin W. Plaxco. "A Super-Sandwich Electrochemical Assay for Sensitive and Selective DNA in Serum and Blood". J. Am. Chem. Soc. 2010. **132**, 14346-14348

(5) Fan Xia, Xiaolei Zuo, Yi Xiao, Di Kang, Alexis Valle-Blisle, Xiong Gong, Alan J. Heeger, Kevin W. Plaxco. "Label-free, Dual-analyte Electrochemical Biosensors: A New Class of Molecular-Electronic Logic Gates". J. Am. Chem. Soc. 2010, **132**, 8557- 8559

(6) Di Kang, Ryan J. White, Alan J. Heeger, Kevin W. Plaxco, Fan Xia, Xiaolei Zuo. "Multi Output surface DNA Based Bio-encoder and Bio-decoder". NPG Asia Mater. 2012, **4**, e1

(7) Di Kang, Alexis Vallee-Belisle, A.Porchetta, Kevin W. Plaxco, Francesco. Ricci. "Re-engineering electrochemical biosensors to narrow or extend their useful dynamic range". Angew. Chem. Int. Ed. 2012, **51**, 6717-6721

(8) Di kang, Ruixue Duan, Yerpeng Tan, Fan Hong, Boya Wang, Zhifei Chen, Shaofang Xu, Xiaoding Lou, Wei Wei, Bernard Yurke, Fan Xia , "Speeding up the self-assembly of a DNA nanodevice using a variety of polar solvents". Nanoscale. 2014, **6**, 14153-14157

(9) Di Kang, Francesco Ricci, Ryan J. White and Kevin W. Plaxco, "A Comparison of Commercially Available or Easily Synthesized Redox Reporters for Application in Electrochemical Biosensors" (in revision)

(10) Di Kang, Sheng Sun, Martin Kurnik, Demosthenes Morales, Fredrick W. Dahlquist and Kevin W. Plaxco, "A new architecture for reagentless, single-step, protein-based electrochemical biosensors" (in preparation)

(11) Di Kang, Jing Yu, Fan Xia, Hongbo Zeng and Kevin W. Plaxco, "Study of surface grafted single strain DNA and double strain DNA by using a surface force apparatus" (in preparation)

(12) Hui Li, Netzahualcóyotl Arroyo, Di Kang, Francesco Ricci, Kevin W. Plaxco, "Drift-corrected, dual-labeled electrochemical aptamer biosensor for continuous, real-time drug detection in undiluted whole blood" (in preparation)

PATENTS

(13) Di Kang, Sheng Sun, Martin Kurnik, Kevin W. Plaxco, "A new architecture for reagentless, single-step, protein-based electrochemical biosensors"

(14) Hui Li, Netzahualcóyotl Arroyo, Di Kang, Francesco Ricci, Kevin W. Plaxco, "Drift-corrected, dual-labeled electrochemical aptamer biosensor for continuous, real-time drug detection in undiluted whole blood"

ABSTRACTS

(15) Martin Kurnik, Netzahualcóyotl Arroyo, Hui Li, Di Kang, Kevin W. Plaxco, "Experimental Measurement of the Thermodynamics Underlying the Surface-Induced Structural Changes of Nucleic Acids and Proteins", 60th annual meeting biophysical society, Los Angeles, USA DOI: http://dx.doi.org/10.1016/j.bpj.2015.11.1172

(16) Martin Kurnik, Netzahualcóyotl Arroyo, Hui Li, Di Kang, Kevin W. Plaxco, "Experimental Measurement of the Thermodynamics Underlying the Surface-Induced Structural Changes of Nucleic Acids and Proteins", 251st American chemical society national meeting, San Diego, USA

FIELDS OF STUDY

Major Field: Biochemistry, Biosensor

Studies on the development and improvement of novel electrochemical biosensors

.

ABSTRACT

Improvement of DNA-Based and Protein-Based Electrochemical Biosensors

by

Di Kang

Recent years have seen the development of a number of reagentless, electrochemical sensors based on the target-induced folding or other target-induced conformational changes in electrode-bound oligo nucleotides, with examples reported to date including sensors for the detection of specific nucleic acids, proteins, small molecules and inorganic ions. These of sensors, termed Electrochemical DNA-based (E-DNA) sensors, are comprised of an electrode modified with surface immobilized, redox-reporter-tagged DNA probes. This technique has emerged as a promising new biosensor platform due to its sensitive and selective measurement of specific molecular targets without the need for additional reagents, wash steps or complex and costly equipment. My thesis work has focused on expanding and improving this increasingly important sensing platform.

To expand the number of signaling DNA probes we can interrogate on a single electrode and to support ratiometric, “error-correcting” sensing we have characterized more than a dozen candidate redox reporters reporting at potentials within the window in which thiol-on-gold self-assembled monolayers are stable. We find, however, that while a handful of reporters, including anthraquinone, Nile blue, and ferrrocene, exhibit reasonable signaling and stability, perhaps disappointingly, only methylene blue exhibits near quantitative stability.

Due to the physics of single-site binging, most biosensors have a fixed dynamic range, which can limit their value. In response, we have developed a simple strategy (analogous to mechanisms employed by nature) to modulate the 'input-output' response of DNA-based receptors systems, which can be adapted to rationally edit the useful dynamic range of our electrochemical DNA sensors. Specifically we have narrowed and broadened the useful dynamic ranges of E-DNA sensors by orders of magnitude, improving the range of analytical problems for which they are suitable.

The number of target molecules that E-DNA sensors can detect is limited by the range of molecules that can be recognized by DNA. Motivated by this we developed an alternative, protein based electrochemical sensor architecture for the detection of protein, peptide and antibody targets that likewise exhibits excellent detection limits without the use of reagents or wash steps. This novel, protein-based electrochemical sensing architecture achieves good specificity and sensitivity, providing a new approach for the quantitative, single-step measurement of specific protein-macromolecule interactions.

Given the importance of surface-bound biomolecules in technologies such as ours, have also performed basic studies of biomolecules on gold surfaces. Specifically, we have used surface forces apparatus (SFA) to study the behavior of surface grafted single-stranded and double-stranded DNAs. Doing so we confirmed the previously proposed "mushroom-like" structure of surface-attached single-stranded DNA, and observed a clear transition from single to double stranded DNA (with the latter exhibiting a rigid rod structure) as the complement is introduced.

TABLE OF CONTENTS

LIST OF FIGURES

LIST OF TABLES

1. Introduction

1.1 Motivation

A biosensor is a device based on the principle of biorecognition and used for the quantitative detection of specific molecules such as drugs, metabolites, peptides, proteins or nucleic acids. To do so the device transduces the biological interaction to an optical or electrical output signal that is easily measured. The ultimate goal of this biosensor is to detect the target accurately (quantatively), conveniently (rapidly and with little or no processing), and inexpensively. To do so it must work in a range of complex samples without requiring sample pretreatment.

The potential applications of biosensors are many, but the challenges are also great. To support rapid (e.g., emergency) clinical diagnoses, doctors must be able to measure health-related molecular markers directly in blood, serum or other bodily fluids. For environmental monitoring, the detection of pesticides, heavy metal ions and other contaminants in raw soil and water samples is the key. For homeland security and defense use, sensors must be fast and support the detection of extremely low levels of pathogens and chemical weapons in air and other complex environmental samples..

The most successful commercial biosensor to date is the blood glucose sensor, an electrochemical platform using the enzyme glucose oxidase to produce an electronic output to monitor blood glucose. The success of the blood glucose meter has lead it to be a model for the development of other biosensors, which strive to be

as convenient and inexpensive. The glucose meter, for example, only requires approximately 1 μL of blood from a finger prick and completes its measurements in just 10 s. The newest glucose sensors can even be implanted under the skin where they continuously deliver glucose measurements for more than a week. These are the attributes that we would like to see in a more general platform, one that can detect essentially any molecular target and not just glucose. Unfortunately, however, the glucose sensor is specific for glucose (due to its use of glucose oxidase) and the approach is not applicable to the detection of most other molecular targets of interest.

Many techniques have been employed in the effort to develop biosensors that, like the glucose sensor, support continuous, real-time detection in the body and yet, unlike the glucose sensor, are generalizable to the detection of almost any target molecule. These techniques include Surface plasmon resonance (SPR), quartz crystal microbalance (QCM) and Field effect transistor based biosensor (Bio-FET). Unfortunately, however, despite years' worth of effort none of these approaches compare to the highly selective performance of the glucose sensor. Those other approaches are just as fast and convenient as the glucose sensor. And they are general, unlike the glucose sensor. The only problem with them is that they are not selective enough to work in blood.

Motivated by the so-far complete lack of generalizable biosensor platforms supporting continuous, real-time measurements in complex sample matrices my thesis work focused on the development and improvement of a new,

electrochemical biosensor platform that couples the selectivity and convenience of the glucose sensor with much broader generalizability. My work was based on the electrochemical DNA sensing platform, an approach that has numerous advantages over SPR, QCM, bio-FET and other adsorption-based approaches. It performs well in realistically complex clinical samples, such as blood serum, plasma or crude cell lysates. Because our sensing technique only sense the signal from binding induced confirmation change; As well as, it is convenient and inexpensive. But it is still limited by several problems. First, there are a few redox reports work in this technique. Second, the useful dynamice range placement and width is fixed; The third, the biorecognition element is limited with DNA and small peptide. The last, however we are successful in applying this technique to make robust sensors, we still not clear understand the physic of the surface grafted biomolecular.

1.2 Electrochemical Biosensors

1.2.1 Biosensors

Clark and Lyon described the first biosensor concept in the early 1960s[1]. In the 50 years since, biosensors has developed into a robust, interdisciplinary field crossing the life sciences, information sciences, chemistry, physics and engineering. Biosensors have been given in-depth attention and are widely needed in the fermentation process, environmental monitoring, food engineering, clinical medicine, and military. To date, the biosensor field has limited success. Not enough biosensor and platform have been developed and commercially used. Most of the developed platforms are absorption based technique; they are likely failed in complex sample. With further improvement, the biosensor will get more and more widely used.

The two key elements of a biosensor are its biomolecular recognition element and its signal transduction mechanism. The recognition element uses biomolecules (proteins, DNA, etc.) to recognize the analyte of interest. In most case, however, this recognition does not produce easy measurable signal. Signal transduction, a physical mechanism that links binding to a measurable physical or chemical change and convert it to a measurable output signal, is thus also a key element of any biosensor architecture.

Molecular recognition is a fundamental part of any biosensor and accounts for much of the enthusiasm for such technologies. The recognition part uses the

biomolacular interaction to specific indentify the analyte from the sample, which requires excellent specificity. For example, to detect a protein from blood serum, there are more than 10,000 proteins presented in serum, and our target is only 1 over 10,000 from this pool. And high sensitivity is another requirement of this component. For example, in a ctDNA detection for a stage I cancer patient in plasma, the total target ctDNA concentration is less than 10 pg/mL. Different biological recognition elements are used in biosensor. The recognition theory includes protein-protein interaction, antibody-antigen binding, enzymes-ligands interaction, DNA or RNA hybridization and DNA or RNA aptamer binding, etc. In general, these biological recognitions have high selectivity and affinity. Because of the complication of the biological system, one potential disadvantage of these recognitions is the binding affinity is very hard to be engineered.

Recognition alone is insufficient to create a biosensor, we still need to transduce the binding event into a measurable output signal. For most biomolecular interactions, however, binding only generates a small change in physics, and thus highly sensitive approaches are needed to read it out. Indeed, most approaches, such as SPR and QCM, are so sensitive that they also produce signals from non-specific binding, limiting their use to unrealistically “clean” samples and preventing their use in the clinic. These approaches include optical sensors, such as surface plasmon resonance, fluorescence polarization, and surface-enhanced raman spectroscopy; mass-based biosensors, such as the quartz crystal microbalance, electronic biosensors, such as those based on field effect transistors; mechanical biosensors,

including microcantilevers and surface acoustic wave sensors; and electrochemical biosensors. Here I review the former as context for the latter.

Surface plasmon resonance (SPR) is a sensitive means of measuring refractive index changes in the vicinity of thin metal layers (i.e., gold, silver, or aluminum films)[2]. The technique is a useful platform in clinical analysis for biomolecular interactions with high sensitivity and without the need of labels by sensing the surface electron field change. Non-specific adsorption, however, also produces a similar signal, and thus target purification is necessary for SPR to work with complex samples, such as blood serum. [3]

Quartz crystal microbalances (QCM) work by sending an electrical signal through a gold-plated quartz crystal, which causes a vibration at its resonant frequency.[4] This frequency changes when the mass of the crystal changes, providing a route to measuring the binding of a biomolecule on the surface of the crystal. This technique is a widely used platform for biomolecular interaction analysis in laboratory settings, where it has proven a useful method for drug screening and protein binding analysis. Because this method is, like SPR, based on measuring absorption to a surface it is very sensitive to non-specific binding, and thus it too only works well in highly pure samples.[4]

Bio-field effect transistor, bio-FET, is transistor the gate surface of which has been modified with biorecognition molecules[5]. When a target molecule binds the charge distribution on the gate is altered, affecting the conductance of the FET. Because it is based on transistors the technique is compact, rapid, inexpensive and

compatible with current circuit fabrication. Its disadvantages, though, are again similar to those of other absorption-based techniques; non-specific adsorption to the sensor surface also alters gating, and thus bio-FETs do not work well when challenged with realistically complex samples[6].

Surface acoustic wave (SAW) sensors are micro-electromechanical devices that employ surface acoustic waves to detect surface changes[7]. Specifically, SAW devices use electrical signal to generate a mechanical surface wave, and then converts the wave back into an electrical signal. Comparison of the input and output electrical signals informs on any surface changes. To convert this into a biosensor the surface is modified with biorecognition molecules, with the sensor measuring the wave change before and after target binding. Once again, this absorption-based technique, which works well in pure sample, fails when challenged with realistically complex samples[7].

Fluorescence polarization, measures the intensity of the emitted light from a polarized light excited fluorophore in vertical and horizontal planes[8]. On the presence of a specific protein-protein binding, the tumbling of an attached fluorophore will change. Because it is single-step (e.g., it does not require washing to remove unbound reagents) and because it is selective enough to employ in modestly complex samples, it has seen the widest use for quantitative diagnostically relevant proteins in point-of-care applications[3, 9-12]. Several limitations, however, significantly reduce the utility of fluorescence polarization. Specifically, its signal gain is relatively small (~15%), and this must be measured against background

polarizations typically ranging from 5 to 10%. Because of this the assay requires significant background subtraction and signal averaging, rendering its overall workflow slow and cumbersome.

In contrast to the above approaches, the most successful biosensor, the blood glucose sensor[13], is an electrochemical biosensor characterized by a highly specific signal transduction mechanism. Fisrt, it is highly selective (not spoofed by non-specific adsorption) due to the specificity of the signal transduction mechanism and the generally low background of electroactive species in clinical samples. Second, it is also very convenient (rapid and single step and continuous). And, it is inexpensive, being based on cheap, hand-held electronics. Unlike SPR, QCM, FP and the other biosensor approaches described above, however, the glucose sensor is not generalizable to arbitrary targets.

1.2.2 The Electrochemical-DNA (E-DNA) Sensing Platform

In our research group, we have developed a new class of electrochemical biosensors, termed Electrochemical DNA (E-DNA) sensors[14, 15]. E-DNA sensors employ square wave voltammetry to monitor the efficiency with which a redox reporter (e.g., methylene blue) attached to a surface-anchored biomolecule approaches an underlying, monolayer-coated gold electrode. Target binding alters this transfer, producing in turn an easily measurable change in Faradic current that is monotonically related to the target concentration. To date the group has developed a series of such biosensors, detecting targets including DNA and RNA, small

molecules, and proteins[16].

The first sensors in this class[14] utilized an oligonucleotide probe to detect specific oligonucleotide targets DNA via hybridization induced changes in the conformation of an electrode bound, single-stranded[15], stem-loop[14] and pseudoknot[17] DNA probe. Using a redox-labeled DNA strand affords extremely specific and selective detection by combining the specificity of DNA hybridization with the highly specific redox chemistry of the electroactive reporter. Given this, it is perhaps not surprising that E-DNA sensors perform well even when challenged with complex, clinically relevant media such as undiluted blood serum, crude cellular extracts, urine and saliva[15].

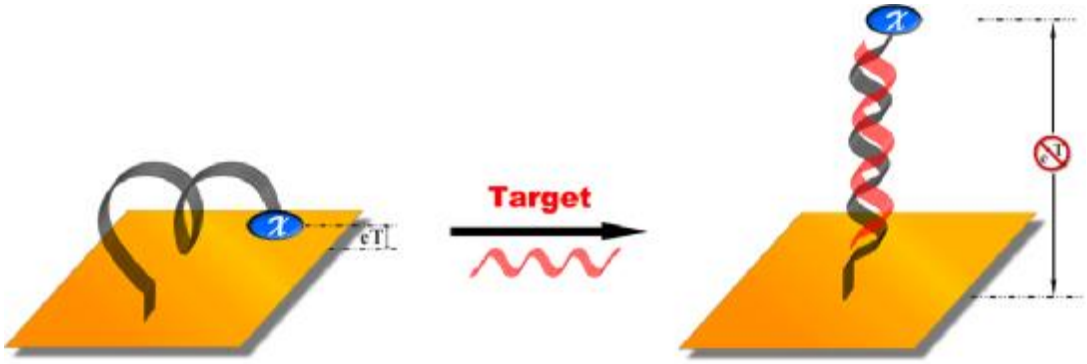

Figure 1-1. Signal generation in the electrochemical DNA (E-DNA) sensor occurs when hybridization with a target oligonuceotide reduces the efficiency with which the attached redox reporter (X) can approach the electrode and transfer electrons.

Electrochemical aptamer-based (E-AB) sensors, which are comprised of an electrode modified with surface immobilized, redox-tagged DNA aptamer (Fig. 1-2), expanded the range of targets that can be detected by the E-DNA platform to proteins,[18-22] small molecules[23-26] and inorganic ions.[27, 28] To do this

E-AB signaling is coupled to binding-induced conformational changes in an electrode-bound aptamer, a DNA or RNA molecule selected in vitro to fold up as a protein does such that it can bind a specific molecular target. This, in turn, results in a readily measurable change in Faradaic current. Not surprisingly, E-AB sensors are likewise insensitive to the non-specific binding of interferants and readily perform when challenged directly in blood serum and other complex sample matrices[29].

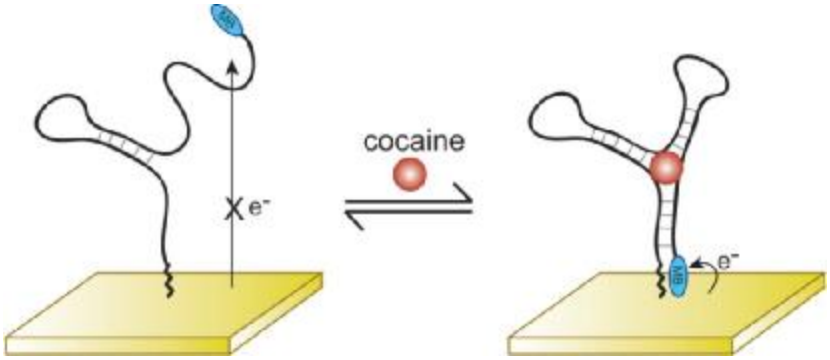

Figure 1-2. The cocaine E-AB sensor is comprised of an unfolded, electrode-bound sensing aptamer. Cocaine binding traps the aptamer in its folded state, forcing an attached redox reporter (here we have employed methylene blue -MB) into proximity with the electrode, leading to a large change in Faradaic current.

Expanding on the E-DNA platform the Plaxco group has also developed an electrochemical approach utilizing a double-stranded nucleic acid "scaffold" modified on one end to present both a protein-recognizing polypeptide or small molecule and a redox reporter and covalently attached to gold electrode via a flexible linker via the other[30]. The binding of the sensor's target to this recognition element reduces the efficiency with which the attached redox reporter approaches the electrode (analogous to the change in tumbling seen in fluorescence polarization), producing an easily measured change in electron transfer efficiency

(analogous to a change in fluorescence polarization). This strategy offers several significant advantages over other methods for detecting protein targets, including the reduced complexity associated with its reagentless, single-step, wash-free format and better performance in complex samples, such as undiluted blood serum and crude soil extracts.

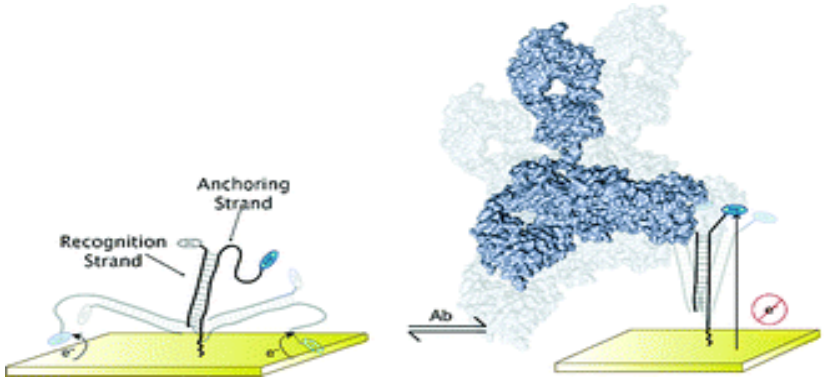

Figure 1-3. The scaffold sensor is us double stranded DNA as a support scaffold for target receptor. At the far end of the double stranded DNA, one strand modified with a redox reporter, and the other strand modified with the target receptor. In absence of target, the redox report collides with electrode surface, which has a larger faradic current. Upon the binding happened, the target antibody reduce the possibility of the redox report collides with electrode surface, which reduce the faradic current.

1.3 The Limitations of Electrochemical DNA Sensors

1.3.1 Limited Number of Redox Reporters

A potential advantage of E-DNA sensors is the ability to deploy multiple receptors on a single electrode via the expedient of employing reporters that signal at distinct, non-overlapping redox potentials. This allows for improved multiplexing and for the introduction of error correcting ratiometric or differential measurement approaches[31, 32]. To date, however, only a limited number of redox reporters

have been used in such sensors and there exists lack of redox reporters with similar stability for ratiometric error correction methods. Only methylene blue exhibits near quantitative stability, which suggests that more effort towards the development of suitable redox reporters is needed if the multiplexing and ratiometric error correction potential of electrochemical biosensors are to be fully realized.

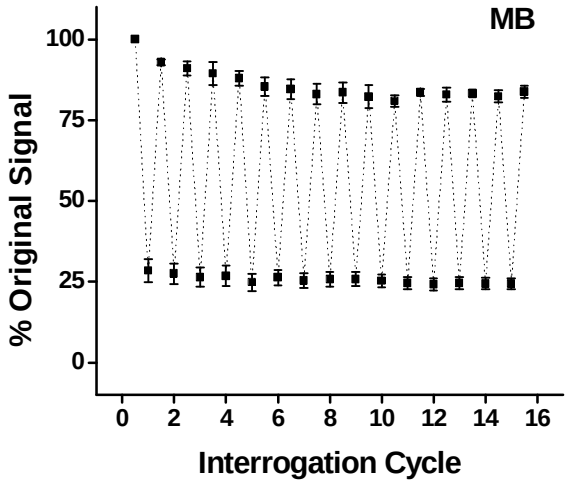

Figure 1-4. Repeated sensor cycling to hybridization and regeneration of a methylene-based sensor demonstrates a mean signal regeneration of 90% per use over 15 cycles. Much of the total loss of signal, however, arises during the first 3 cycles; the sensor exhibits a mean recovery of 98% per iteration after these steps. The sensor signal is also highly reproducible, producing a mean signal suppression of 74 ± 1.3 % when challenged with a fully complementary target.

1.3.2 Fixed Dynamic Range

While the versatility, specificity and often impressive affinity of biomolecular recognition has, as noted above, motivated decades of research aimed at the development of sensors based on the effect, biomolecular receptors are not without potentially important limitations in such applications. Key among these for some

applications is the fact that the useful dynamic range (here defined as the range from 10% signal change to 90% signal change) is fixed both in terms of its placement and its width. Misalignment between the placement of this range and the expected range of target concentrations reduces both sensitivity and specificity. Specifically, the useful dynamic range of single-site receptors typically spans a fixed, 81-fold change in target concentration, which is a potential limitation biosensors. For example, in some applications, such as viral load monitoring, which requires monitoring a range much wider than 80 fold, it will be nice to have a wide dynamic range. In some other applications, such as monitoring drugs with narrow therapeutic windows, it requires highly sensitive detection. To measure these small changes in target concentration, 81 fold dynamic range it too wide to precision. In order to make our sensor more useful, turning the dynamic range becomes more and more important.

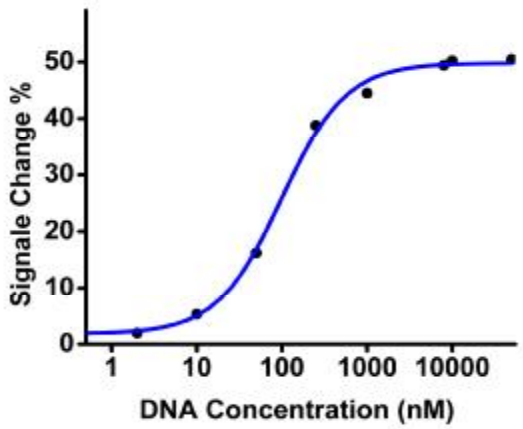

Figure 1-4. The binding curve of a typical single-site receptor is show. The useful dynamic range (defined here as the range from a 10% sensor response to a 90% response) spans an 81-fold change in concentration (here from 10 nM to 810 nM target concentration) that is

centered on the receptor's dissociation constant. The fixed placement and fixed width of this dynamic range are difficulties for some applications, as the best precision and specificity are seen when the useful dynamic range closely matches the expected range of target concentrations, and the best precision and greatest convenience are realized when the width of the useful dynamic range parallels the width of the expected concentration range.

1.3.3 Limited Range of Targets

To date the E-DNA platform has been expended from its original architecture, for the detection of DNA[14], to sensors for the detection of a range of protein and small molecule targets[16]. In the first round, this expansion was driven by the introduction of aptamers, which are lab selectived biomolecule to specify binding with its target. The selection process, by which new aptamers are created, however, appears a limiting step for the further expansion of sensors in this class. First, not all interesting target molecules are amenable to binding by aptamers. Second, the specificity of aptamers is likely poorer than that of proteins due to the higher chemical complexity of proteins. In response, the Plaxco group developed "scaffold "sensors[30]. The probe is a piece of redox reportor modified double stranded DNA, one end fixed on the surface, and the other end coupled a small molecule or peptide. When the target binds to the probe molecule, it reduce the DNA tumbling on the surface. A limitation of scaffold sensors is that, due to their mechanism, they will fail if the attached biorecognition segment is too large, limiting these to short polypeptides. The development of an analog employing a full-length proteins would thus likely greatly extend the range of our electrochemical approach.

1.3.4 Limited Understand of the Physics of Biopolymers on Surfaces

Surface-attached biomolecules play important roles throughout biology and engineering, with examples of the latter including DNA microarrays, biosensors and drug delivery vehicles. Despite their importance, however, our understanding of physics of surface-bound biomolecules remains in its infancy, with most of the rather limited literature reported to date having focused on the behavior of long DNA molecules grafted on surface, with the quantitative characterization of more technologically relevant short DNAs on well-defined surfaces remaining quite limited[33, 34]. This distinction is significant, because in the limit of short chain lengths (and DNAs that fold into complex 3-dimensional structures) polyelectrolyte scaling theories are no longer applicable. There thus exists an important need to better understand the behavior of short single- and double-stranded DNA structures on surfaces as such would improve our ability of rational optimization of the surfaces used in biomolecule-based technologies.

1.4 Reference

1. Clark, L.C. and C. Lyons, *Electrode Systems for Continuous Monitoring in Cardiovascular Surgery.* Annals of the New York Academy of Sciences, 1962. **102**(1): p. 29-&.
2. Homola, J., *Present and future of surface plasmon resonance biosensors.* Analytical and Bioanalytical Chemistry, 2003. **377**(3): p. 528-539.
3. Nguyen, H.H., et al., *Surface Plasmon Resonance: A Versatile Technique for Biosensor Applications.* Sensors, 2015. **15**(5): p. 10481-10510.
4. Rickert, J., A. Brecht, and W. Gopel, *Quartz crystal microbalances for quantitative biosensing and characterizing protein multilayers.* Biosensors & Bioelectronics, 1997. **12**(7): p. 567-575.
5. Brand, U., et al., *Monitoring and Control of Biotechnological Production Processes by Bio-Fet-Fia-Sensors.* Applied Microbiology and Biotechnology, 1991. **36**(2): p. 167-172.
6. Rajan, N.K., X.X. Duan, and M.A. Reed, *Performance limitations for nanowire/nanoribbon biosensors.* Wiley Interdisciplinary Reviews-Nanomedicine and Nanobiotechnology, 2013. **5**(6): p. 629-645.
7. Lange, K., B.E. Rapp, and M. Rapp, *Surface acoustic wave biosensors: a review.* Analytical and Bioanalytical Chemistry, 2008. **391**(5): p. 1509-1519.
8. Dandliker, W.B., et al., *Fluorescence Polarization Immunoassay - Theory and Experimental Method.* Immunochemistry, 1973. **10**(4): p. 219-227.
9. Melanson, S.E.F., *Implementing Drug-of-Abuse Testing at the Point of Care:*

Device Characteristics and Decision Criteria With Selected Emphasis on the Biosite Triage System. Point of Care, 2005. **4**(3): p. 123-127.

10. von Lode, P., *Point-of-care immunotesting: Approaching the analytical performance of central laboratory methods.* Clinical Biochemistry, 2005. **38**(7): p. 591-606.
11. Jameson, D.M. and J.A. Ross, *Fluorescence Polarization/Anisotropy in Diagnostics and Imaging.* Chemical Reviews, 2010. **110**(5): p. 2685-2708.
12. Lea, W.A. and A. Simeonov, *Fluorescence polarization assays in small molecule screening.* Expert Opinion on Drug Discovery, 2011. **6**(1): p. 17-32.
13. Updike, S.J. and G.P. Hicks, *Enzyme Electrode.* Nature, 1967. **214**(5092): p. 986-&.
14. Fan, C.H., K.W. Plaxco, and A.J. Heeger, *Electrochemical interrogation of conformational changes as a reagentless method for the sequence-specific detection of DNA.* Proceedings of the National Academy of Sciences of the United States of America, 2003. **100**(16): p. 9134-9137.
15. Lubin, A.A., et al., *Sequence-specific, electronic detection of oligonucleotides in blood, soil, and foodstuffs with the reagentless, reusable E-DNA sensor.* Analytical Chemistry, 2006. **78**(16): p. 5671-5677.
16. Lubin, A.A. and K.W. Plaxco, *Folding-Based Electrochemical Biosensors: The Case for Responsive Nucleic Acid Architectures.* Accounts of Chemical Research, 2010. **43**(4): p. 496-505.

17. Cash, K.J., et al., *Optimization of a Reusable, DNA Pseudoknot-Based Electrochemical Sensor for Sequence-Specific DNA Detection in Blood Serum.* Analytical Chemistry, 2009. **81**(2): p. 656-661.

18. Willner, I. and M. Zayats, *Electronic Aptamer-Based Sensors.* Angewandte Chemie International Edition, 2007. **46**(34): p. 6408-6418.

19. Josep Lluis, A.S., Eva Baldrich, Abd El-Gawad Radi, Srujan Dondapati, Pablo Lozano Sanchez, Ioanis Katakis, Ciara K. O'Sullivan, *Electronic ?Off-On? Molecular Switch for Rapid Detection of Thrombin.* Electroanalysis, 2006. **18**(19-20): p. 1957-1962.

20. Yi Xiao, A.A.L., Alan J. Heeger, Kevin W. Plaxco, *Label-Free Electronic Detection of Thrombin in Blood Serum by Using an Aptamer-Based Sensor.* Angewandte Chemie International Edition, 2005. **44**(34): p. 5456-5459.

21. Xiao, Y., et al., *A Reagentless Signal-On Architecture for Electronic, Aptamer-Based Sensors via Target-Induced Strand Displacement.* J. Am. Chem. Soc., 2005. **127**(51): p. 17990-17991.

22. Lai, R.Y., K.W. Plaxco, and A.J. Heeger, *Aptamer-Based Electrochemical Detection of Picomolar Platelet-Derived Growth Factor Directly in Blood Serum.* Anal. Chem., 2007. **79**(1): p. 229-233.

23. Baker, B.R., et al., *An Electronic, Aptamer-Based Small-Molecule Sensor for the Rapid, Label-Free Detection of Cocaine in Adulterated Samples and Biological Fluids.* J. Am. Chem. Soc., 2006. **128**(10): p. 3138-3139.

24. Zayats, M., et al., *Label-Free and Reagentless Aptamer-Based Sensors for*

Small Molecules. J. Am. Chem. Soc., 2006. **128**(42): p. 13666-13667.

25. Zuo, X., et al., *A Target-Responsive Electrochemical Aptamer Switch (TREAS) for Reagentless Detection of Nanomolar ATP.* J. Am. Chem. Soc., 2007. **129**(5): p. 1042-1043.

26. Ferapontova, E.E., E.M. Olsen, and K.V. Gothelf, *An RNA Aptamer-Based Electrochemical Biosensor for Detection of Theophylline in Serum.* J. Am. Chem. Soc., 2008.

27. Xiao, Y., A.A. Rowe, and K.W. Plaxco, *Electrochemical Detection of Parts-Per-Billion Lead via an Electrode-Bound DNAzyme Assembly.* J. Am. Chem. Soc., 2007. **129**(2): p. 262-263.

28. Radi, A.-E. and C.K. O'Sullivan, *Aptamer conformational switch as sensitive electrochemical biosensor for potassium ion recognition.* Chemical Communications, 2006(32): p. 3432-3434.

29. Xiao, Y., et al., *Label-free electronic detection of thrombin in blood serum by using an aptamer-based sensor.* Angewandte Chemie-International Edition, 2005. **44**(34): p. 5456-5459.

30. Cash, K.J., F. Ricci, and K.W. Plaxco, *An Electrochemical Sensor for the Detection of Protein-Small Molecule Interactions Directly in Serum and Other Complex Matrices.* Journal of the American Chemical Society, 2009. **131**(20): p. 6955-+.

31. Kang, D., et al., *DNA biomolecular-electronic encoder and decoder devices constructed by multiplex biosensors.* Npg Asia Materials, 2012. **4**.

32. Du, Y., et al., *Reagentless, Ratiometric Electrochemical DNA Sensors with Improved Robustness and Reproducibility.* Analytical Chemistry, 2014. **86**(15): p. 8010-8016.

33. Anne, A., A. Bouchardon, and J. Moiroux, *3 '-ferrocene-labeled oligonucleotide chains end-tethered to gold electrode surfaces: Novel model systems for exploring flexibility of short DNA using cyclic voltammetry.* Journal of the American Chemical Society, 2003. **125**(5): p. 1112-1113.

34. Petrovykh, D.Y., et al., *Nucleobase orientation and ordering in films of single-stranded DNA on gold.* Journal of the American Chemical Society, 2006. **128**(1): p. 2-3.

2. A survey of redox-active moieties for application in multiplexed electrochemical biosensors highlights the need for improved redox reporters[1]

2.1 Abstract

Recent years have seen the development of a large number of electrochemical sensors employing biomolecules modified via the attachment of a redox-active "reporter." A potential advantage of these sensors is the ability to deploy multiple receptors on a single electrode via the expedient of employing reporters that signal at distinct, non-overlapping redox potentials. This allows for improved multiplexing and for the introduction of error correcting ratiometric or differential measurement approaches. To date, however, only a limited number of redox reporters have been used in such sensors. In response we characterize here the performance of more than a dozen of potential reporters that are, first, redox active within the potential window over which (commonly employed) thiol-on-gold monolayers are stable and, second, commercially available in forms that are either readily conjugated to biomolecules or can be converted into such forms in one or two simple synthetic steps. To test each of these reporters we conjugated it to one terminus of a single-stranded DNA "probe" that was attached by its other terminus to a gold

[1] This chapter was adapted from a research article submitted for publication in Analytical Chemistry. Reproduced in part with permission from [Kang et al. A survey of redox-active moieties for application in multiplexed electrochemical biosensors highlights the need for improved redox reporters. *Anal. Chem.,* **2016**, Submitted]

electrode to form an “E-DNA” sensor responsive to its complementary DNA target. We then measured the signaling properties of each sensor and its stability against repeated voltammetric scans and against deployment in and reuse from blood serum. We find that while a handful of reporters, including anthraquinone, Nile blue, and ferrrocene, exhibit reasonable signaling and stability, perhaps disappointingly, only methylene blue exhibits near quantitative stability. Our work thus serves as both a cautionary tale –we wish to help other researchers avoid fruitless efforts to employ the many, seemingly promising and yet ultimately inadequate reporters we have investigated- and as an illustration of the pressing need for the further development of useful redox reporters.

2.2 Introduction

Due to the ease, with which they are fabricated and employed, and their oft-impressive selectivity and detection limits, electrochemical biosensors employing redox-reporter-modified oligonucleotides[1] and polypeptides[2] have seen significant recent attention. The potential advantages of sensors in this class are multiple. First, they achieve good detection limits without the use of wash steps or the addition of exogenous reagents[3-5]. Second, they perform well even when deployed directly in realistically complex clinical samples, such as blood serum, saliva, or crude cell lysates[6-8], and have even been used for the continuous measurement of plasma drug levels[9]. Third, sensor fabrication is facile[10], and the electronics required to interrogate these sensors are convenient and inexpensive[11].

In addition to the above, an additional advantage of this class of electrochemical biosensors is the ability to deploy multiple sensors on a single electrode by employing reporters that signal at unique, non-overlapping reduction potentials. This allows for improved multiplexing[12,13] and for the introduction of error correcting, ratiometric measurement approaches[14,15]. To date, however, the literature describing these sensors has almost entirely utilized methylene blue6, Nile blue[16,17], anthraquinone[18], or ferrocene[4,19] as reporters. The expansion of this relatively short list could improve the extent to which such sensors can be multiplexed. Moreover, we have found (data not shown) that a lack of redox reporters of similar stability hinders ratiometric error correction methods, which suffer if one reporter degrades more rapidly than the other. Motivated by these observations we have, over many

years of work in this area, characterized more than a dozen candidate redox reporters, all of which are either commercially available in forms easily conjugated to biomolecules or are readily converted into such forms via one or two simple synthetic steps and all of which are active at potentials within the window in which thiol-on-gold self-assembled monolayers are stable. As shown here, however, very few of these potential reporters exhibit acceptable stability, and thus we abandoned almost all of them without reporting their characterization in the literature. Recently, however, we have become aware that other researchers had similarly characterized and found unsuitable many of the same potential reporters. In an effort to help future researchers avoid repeating yet again these same studies (none of which have previously been published, thus causing unnecessary repetition of effort), and to hopefully motivate efforts to identify new redox reporters, we describe here these largely "negative" results.

2.3 Results and discussion

The commercially available or easily synthetically accessible redox reporters we have characterized fall into either of two classes: organic small molecules and organometallic complexes. Among the former we have characterized methylene blue, thionine, anthraquinone, anthraquinone with a five-carbon linker (anthraquinone-C5), gallocyanine, Nile blue, indophenol, neutral red, dabcyl, and carboxy-X-rhodamine (ROX) (Fig. 2-1). Among the latter we have characterized ferrocene attached directly to either the 5' or 3' end of the DNA, ferrocene linked to the DNA via a five-carbon linker (ferrocene-C5), and pentamethylferrocene. All told we have, over more than a decade of working in the field of electrochemical biosensors, characterized more than a dozen potential redox reporters, each as with a carboxylic acid group supporting ready conjugation to an amine-terminated DNA. Here we summarize the results of our many years' experience working with these potentially promising reporters.

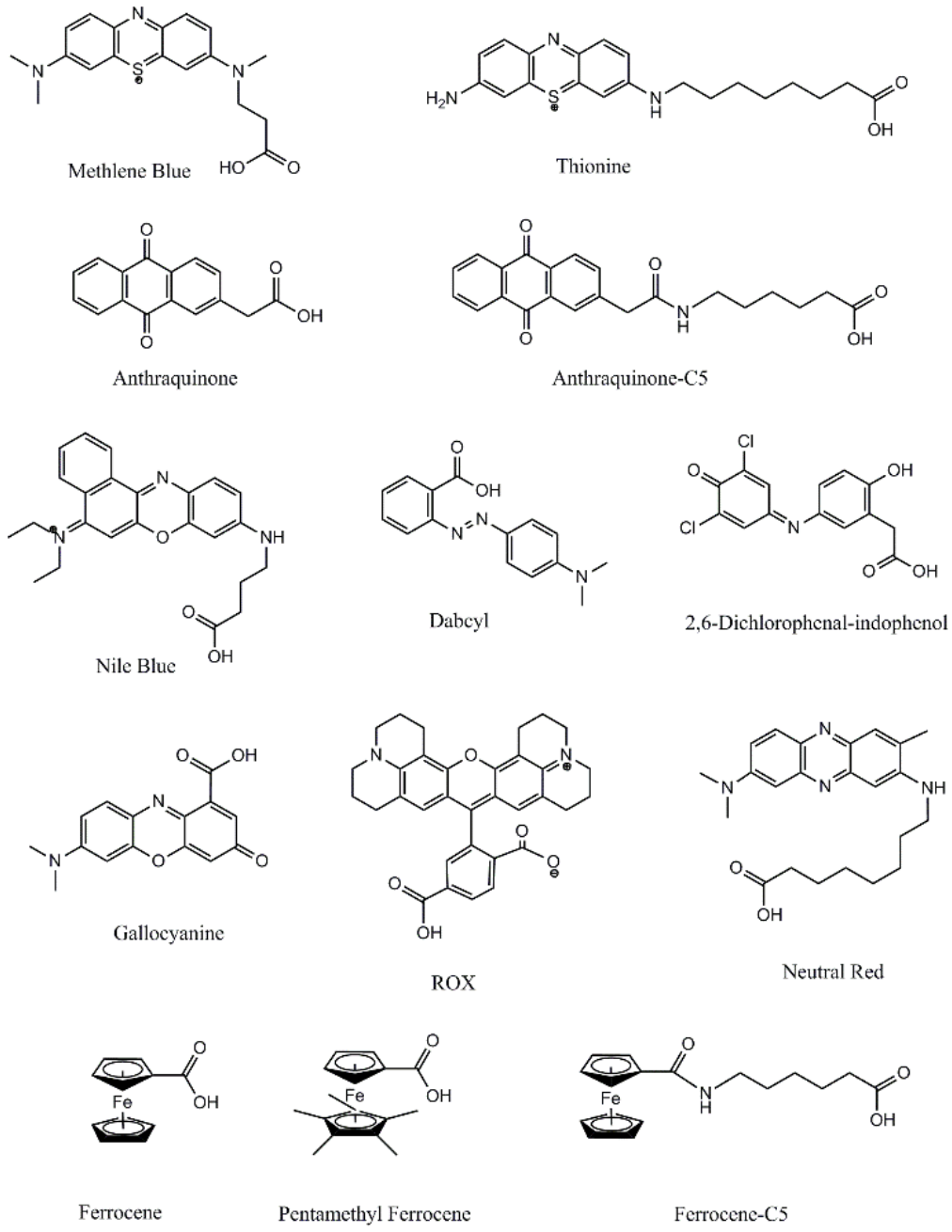

Figure 2-1. We characterized 13 potential redox reporters in total, nine organic small molecules and two organometallic complexes. Two of these, ferrocene and anthraquinone, were investigated with and without an additional five-carbon linker and one, ferrocene, was investigated using both 3' and 5' linkages. All these potential reporters are available in (or are easily synthesized as) forms containing a carboxylic acid group for ready conjugation to an amine-modified DNA.

To characterize the utility of these commercially or easily synthetically available redox reporters we have, over a number of years of research incorporated each into a simple E-DNA electrochemical DNA sensors. Specifically, we employed E-DNA sensors composed of linear DNA strands modified with the relevant redox reporter on its 3'-terminus (except for ferrocene, for which we have explored two 3' and one 5' linkage) and attached at its opposite terminus to a six-carbon alkane thiol monolayer to a gold electrode [21]. Hybridization with a target oligonucleotide reduces the efficiency with which the attached redox reporter transfers electrons to the interrogating electrode, leading to a significant decrease in faradaic current when the system is interrogated using, for example square wave voltammetry. For each of the resulting sensors we measured signaling (i.e., do we see a clear, single oxidation and reduction peaks for the DNA-reporter conjugate), signal gain (relative signal change upon target saturation), electrochemical reversibility (i.e., its stability against multiple voltammetric scans) and stability when exposed to a realistically complex sample matrix (20% blood serum).

The properties of the potential reporters we have characterized vary widely. For example, three of the potential reporters, thionine, dabcyl and ROX, failed to produce clear oxidation and reduction peaks when conjugated to DNA (Fig. 2-2a). A fourth potential reporter, indophenol, proved difficult for conjugation to DNA. Specifically, although free indophenol carboxylic acid is stable (and electrochemically active) under basic conditions we found that it decomposed during our attempts to conjugate it to an amine-terminated DNA. The redox

potential of a fifth candidate, neutral red, shifts to -0.7 V when modified to support DNA conjugation, moving its potential close to the redox potential of alkane thiols on gold and rendering the resultant sensor unstable (data not shown). Finally, a sensor employing a 3' ferrocene reporter produced only a very small peak current (Fig. 2-2), and thus we decide not to carry it over to our next testing step. The remaining reporters, in contrast, are all easily conjugated to amine-modified DNA and produce clear redox peaks within the potential window over which alkane-thiol-on-gold self-assembled monolayers are stable.

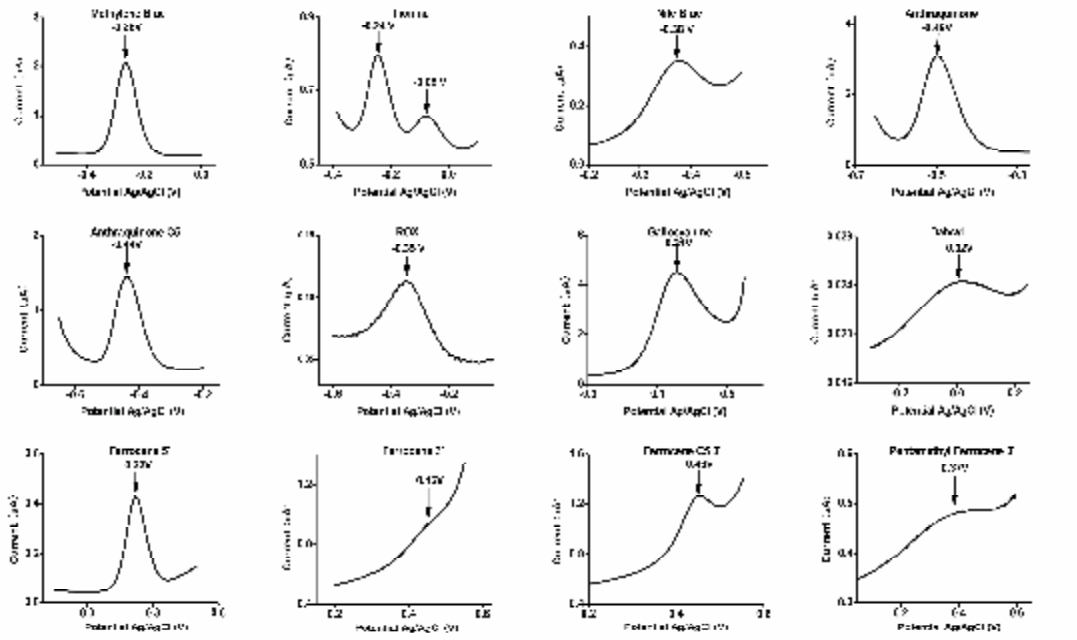

Figure 2-2. Not all redox reporters are created equal. Dabcyl and ROX, for example, fail to produce clear oxidation and reduction peaks when conjugated to DNA and interrogated using our standard square wave voltammetric parameters, and thionine exhibits two peaks in the relevant potential window. We investigated three ferrocene-containing constructs: one in which the ferrocene is conjugated directly on to an amine appended to the 5' end of the DNA, a second in which the ferrocene is conjugated directly on to an amine appended to the 3' end of the DNA, and a third, ferrocene C5, in which there is an additional spacer between ferrocene and the amide linkage to the DNA.

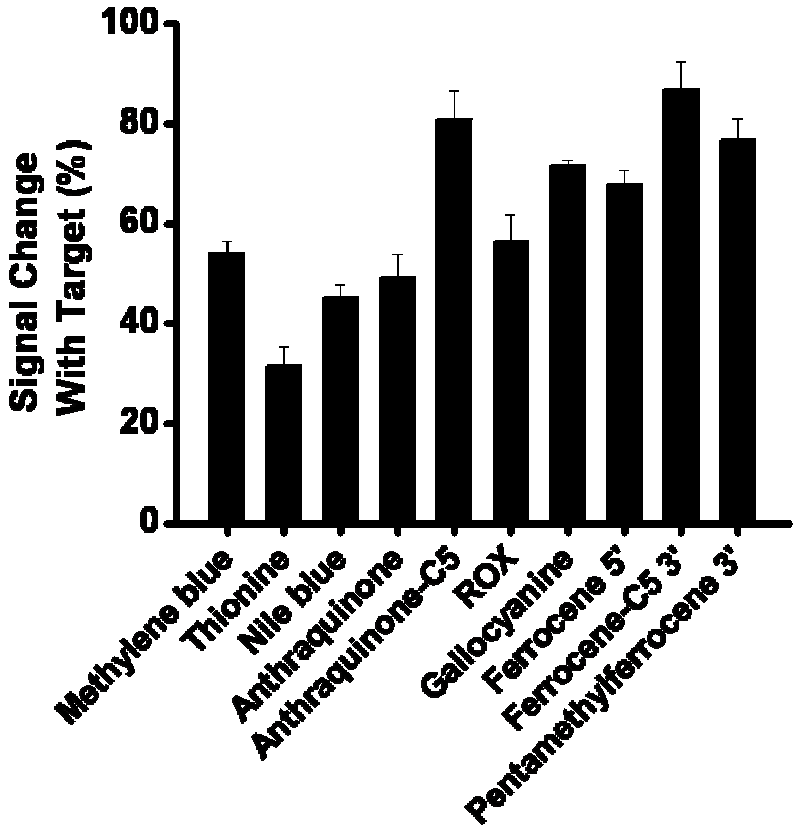

Figure 2-3. We challenged the reporter-conjugated probes that exhibit clear reduction and oxidation peaks with saturating concentrations of their complementary target to test their signaling properties. All respond as expected to these targets, albeit with varying signal gain. Of note signal gain in this class of sensors is a strong function of both the intrinsic electron transfer rate of the reporter and the square wave frequency and amplitude, thus likely accounting for the variations in signal gain observed (all data were collected under a single set of square wave parameters).

All of the remaining redox-reporters in our set produce at least reasonably high-gain E-DNA sensors under the standard volammetric parameters we employ in our sensors (Fig. 2-3). The stability of the resultant sensors to repeated oxidation-reduction cycles, however, varies widely (Fig. 2-4). Sensors fabricated with methylene blue, for example, are impressively stable, exhibiting only 2%

current loss after 100 square-wave voltammetric scans in buffer. Sensors employing anthraquinone, Nile blue or 5'-linked ferrocene, in contrast, are only modestly stable under these conditions, exhibiting ~50% signal loss after 100 scans. Sensors fabricated using 3'-linked ferrocene, ferrocene-C5 and penta-methyl ferrocene linked are still less stable, loosing ~50% of their initial signal after only 50 scans. For most of the sensors we observe an exhibit steady, monotonic decrease in current as the number of scans increases. The signaling current of anthraquinone-based sensors, however, drops off rapidly during the first few scans before largely leveling off, and the signaling current from the gallocyanine-based sensor increases significantly upon repeated scanning. The origins of this increase are unknown to us.

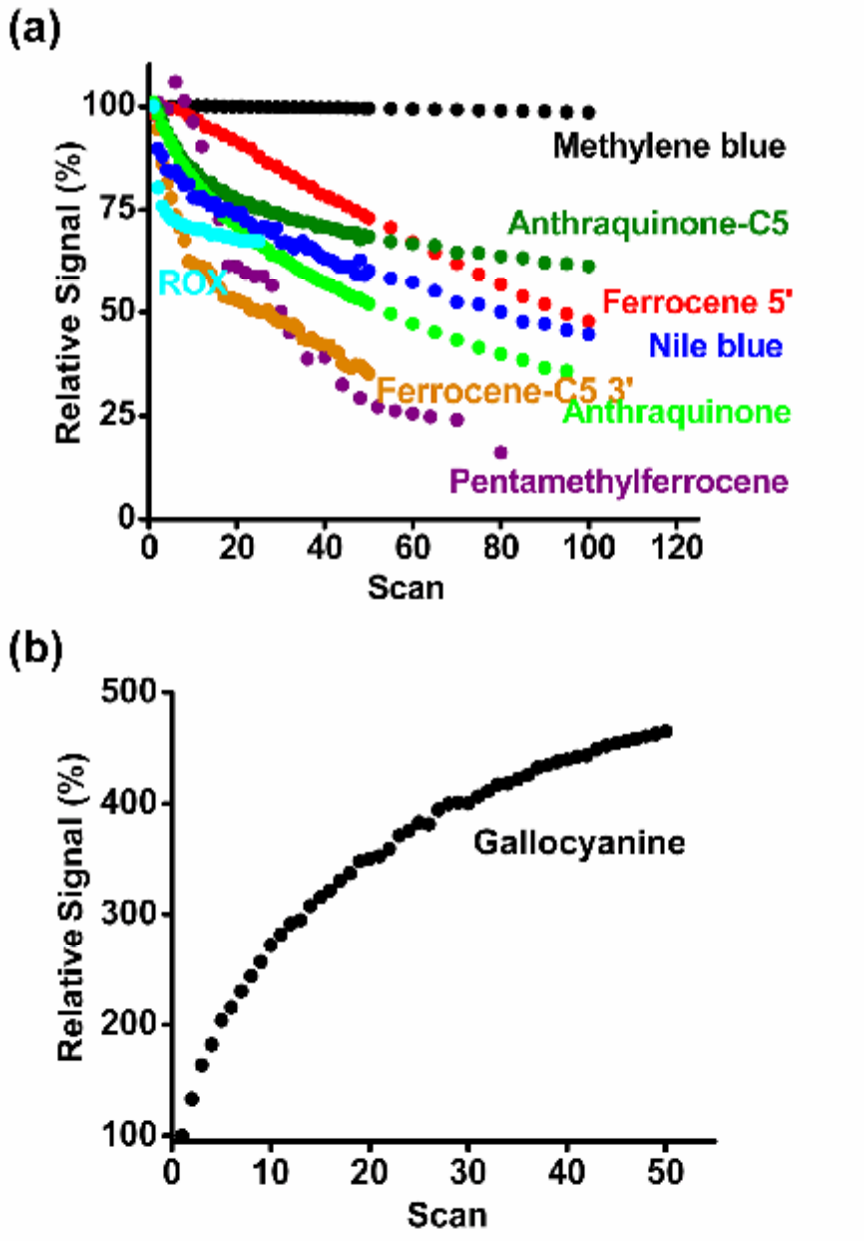

Figure 2-4. With the notable exception of methylene blue, (a) the redox reporters we have investigated are at least somewhat unstable against repeated voltammetric scans, here conducted in phosphate/NaCl buffer. (b) Unlike the other reporters we have characterized, the signaling current from gallocyanine-based sensors increases upon repeated scanning.

An advantage of E-DNA-type sensors is their performance in complex sample matrices such as blood serum[1]. Thus motivated we have tested the performance of sensors fabricated using the reporters (methylene blue, 5'-ferrocene, anthraquinone, and Nile blue) when deployed in 20% blood serum. The gain of each is effectively indistinguishable from that seen in simple buffer solutions (Fig. 2-5a). And, once again, we find that methylene blue is quite stable, exhibiting only minor signal loss when scanned twice an hour for more than 8 hr under these conditions (Fig. 2-5b). Sensors employing 5'-ferrocene, anthraquinone, or Nile blue, in contrast, loose 25-30% their original signal under these same conditions. Oddly, sensors fabricated with anthraquinone exhibit significant signal loss during the first 90 min under these conditions before then exhibiting a slow increase in signal. Finally, methylene blue-based sensors exhibit only 11% decay over four cycles of deployment in serum followed by regeneration (Fig. 2-5c). Nile blue-based sensors, in contrast, exhibit 20% loss and anthraquinone- and ferrocene-based sensors exhibit about 50% losses under these same use-and-regeneration conditions.

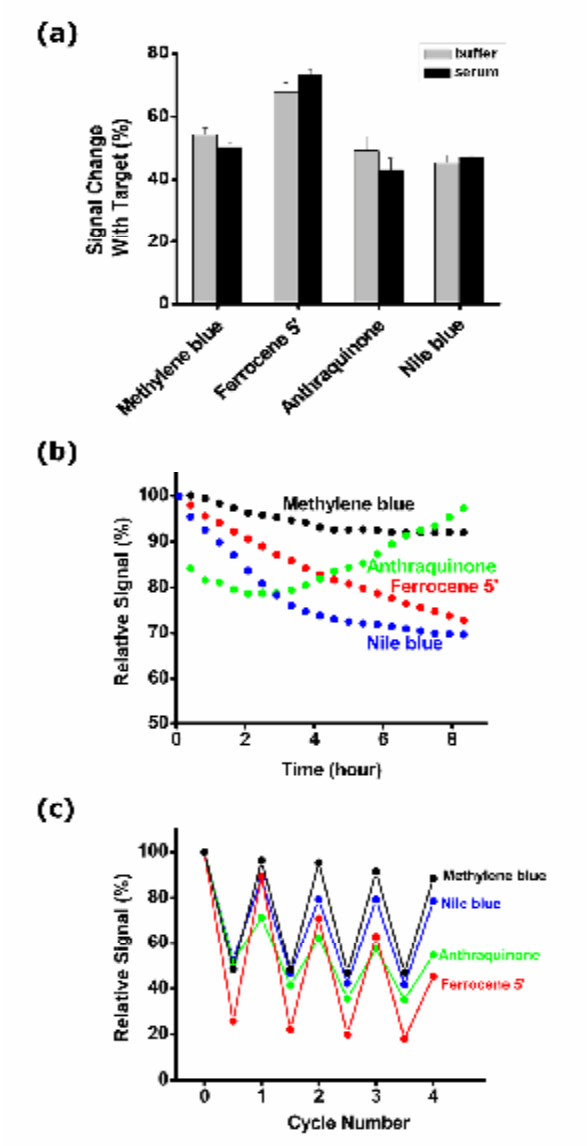

Figure 2-5. We characterize the performance of methylene blue, ferrocene, anthraquinone and Nile blue in 20% blood serum. (a) Sensors fabricated with methylene blue, ferrocene, anthraquinone or Nile blue exhibit similar signal gain in response to target binding whether deployed in simple buffer solutions or in 20% blood serum. (b) They all drift significantly, however, when repeatedly scanned in 20% serum over the course of hours, with methylene blue exhibiting the least drift. The pronounced biphaseic (downward and then upward) drift of anthraquinone reflects the highly variable drift properties of this reporter in serum (i.e., the drift varies dramatically from trial to trial). Similar trial-to-trial variability is seen for the drift of methylene blue-based sensors when challenged in undiluted whole blood (data not shown). Its origins are unclear. (c) Methylene blue-based sensors are likewise the most stable when the sensors are challenged with multiple cycles of hybridization (with saturating target) and regeneration (via di-water wash) in 20% blood serum.

Here we have shown that, although a number of redox active moieties that are available in forms easily conjugated to DNA also support high-gain E-DNA signaling, the stabilities of the resulting sensors differ dramatically. Sensors employing methylene blue, for example, exhibit outstanding stability even in a complex, multi-component sample matrix. The next best reporters, in contrast, including ferrocene, anthraquinone, and Nile blue, also produce high-gain sensors but exhibit rather significantly poorer stability against repeated voltammetric scanning. Together these results suggest that more effort towards the development of suitable redox reporters is needed if the multiplexing and ratiometric error correction potential of electrochemical biosensors are to be fully realized.

2.4 Experiment and Method

Reagents

Anhydrous ferrous chloride (Sigma-Aldrich), sodium nitrite (Sigma-Aldrich), Sodium cyclopentadienide (Sigma-Aldrich), n-butyllithium (1.6 M in n-hexane) (Sigma-Aldrich), pentamethylcyclopentadiene (Sigma-Aldrich), 2-chlorobenzoyl chloride (Sigma-Aldrich), aluminum chloride (Sigma-Aldrich), potassium t-butoxide (Sigma-Aldrich), methyl tertiary butyl ether (Sigma-Aldrich), ferrocene-carboxylic acid, N-hydroxysuccinimide (Sigma-Aldrich), N-hydroxysulfosuccinimide sodium salt (NHS), N-(3-dimethyl-amino-propyl)-N'-ethylcarbodiimide (Fluka), 2,6-dichloro-p-benzoquinone-4-chloroimine (Fisher), 2-hydroxyphenylacetic acid (Fisher), Neutral red (Sigma-Aldrich), 3,7-bis(N-(3-carboxypropyl)-N-methylamino)-phenothiazin-5-ium perchlorate (MB -NHS, empBiotech GmbH), anthraquinone-NHS (AQ-NHS, empBiotech GmbH), anthraquinone-2-amidopentyl carboxylic acid NHS ester (empBiotech GmbH), gallocyanine carboxylic acid NHS ester (empBiotech GmbH), ferrocene-amidopentyl carboxylic acid NHS ester (empBiotech GmbH), phosphate buffer (Sigma-Aldrich), 4-(2-hydroxyethyl)-1-piperazineethanesulfonic acid (HEPES) (Sigma-Aldrich) and fetal calf serum (Sigma-Aldrich) were all used as received.

For the majority of our studies we employed this sequence as our E-DNA "probe."

5'–HS-$(CH_2)_6$–TGGATCGGCGTTTTATT-$(CH_2)_6$–NH_2–3'

which we conjugated in-house to carboxyl-modified reporters it to form an amide bond (see below). Five of the potential reporters we characterized, however, were instead obtained as DNA conjugates directly from a commercial synthesis house (Biosearch, Inc., Novato, CA):

5'–HS-$(CH_2)_6$–TGGATCGGCGTTTTATT–$(CH_2)_6$–(NH-CO)-ROX–3'

5'–HS-$(CH_2)_6$–TGGATCGGCGTTTTATT–$(CH_2)_6$–(NH-CO)-dabcyl–3'

5'–HS-$(CH_2)_6$–TGGATCGGCGTTTTATT–$(CH_2)_6$–(NH-CO)-anthraquinone–3'

5'–HS-$(CH_2)_6$–ATTATTGATCGGCGTTTTAAAGAAG–$(CH_2)_6$–(NH-CO)-methylene blue–3′

3'–HS-$(CH_2)_6$–AGACAAGGAAAATCCTTCAATGAAGTGGGTCG–$(CH_2)_6$–(NH-CO)-ferrocene-5'

As the target oligonucleotide for these sensors we employed the following unmodified DNA constructs as appropriate:

5'–AATAAAACGCCGATCCA–3'

5'–TAAAACGCCGATC–3′

5'–CGACCCACTTCATTGAAGGATTTTCCTTGTCT–3'

Synthesis of Succinimidyl Ester-modified redox reporters

Thionine. We mixed thionine (2.6 g) and 8-bromooctanoic acid (3 g) in DMF (40 mL) to synthesis 3N-octanoic-acid-modified thionine. The mixture was refluxed overnight (10 hr). The crude product mixture was concentrated in vacuum, before being dissolved in methanol and filtered (Celite). We use silica column

chromatography (100:12:1.2 with chloroform/methanol/acetic acid) to purify the product (251 mg) with poor yield (7.5%).

To synthesize thionine succinimidyl ester, we mixed N,N'-Dicyclohexylcarbodiimide (DCC), N-hydrosuccinamide (NHS), and 3N-octanoic-acid-modified thionine in dry dimethylformamide (DMF). The solution was stirred overnight under argon at room temperature. We concentrated the mixture in vacuum, and purified the product with silica column chromatography (100:12:1.2 chloroform/methanol/acetic acid).

Nile Blue. We first prepared 5-(dimethylamino)-2-nitrosophenol by dissolving 826 mg of 3-(dimethylamino)phenol in concentrated hydrochloric acid (5 mL) at 0ºC, followed by the slow addition of 400 mg sodium nitrite, stirring until the content solidified (about 40 min). The precipitate was isolated via vacuum filtration and washed with chilled 1 M hydrochloric acid. The crude product, a yellow-brown solid, was dried in vacuum and used for the conjugation reaction without further purification. In parallel we prepared 3-(naphthalen-1-ylamino) propanoic acid by dissolving 200 mg naphthylamine in DMF (15 mL) followed by the addition of 5 mL of 6 M sodium hydroxide and equimolar amounts of dissolved 3-bromo-propionic acid ethyl ester. We refluxed the mixture for 12 hr. After the reaction finished, we dried the crude reaction mixture in vacuum and purify the product using silica column chromatography (20:1 hexane/methanol). To obtain propionic acid modified Nile blue we first dissolved 34 mg of 5-(dimethylamino)-2-nitrosophenol and 44 mg of

3-(naphthalen-1-ylamino)propanoic acid in DMF (10 mL), and heated the reaction mixture to 90ºC for overnight. We dried the crude reaction mixture in vacuum and purified it using silica column chromatography (3:1 $CHCl_3$/methanol).

2,6-Dichlorophenal-indophenol. We dissolved 150 mg 2,6-dichloro-p-benzoquinone-4-chloroimine in 2 mL methanol and 2-hydroxyphenylacetic acid in 10 mL 100 mM K_2HPO_4. We then mixed two solutions and stirred overnight at room temperature. The resulting solution was dried under vacuum to produce the crude purple blue product which we purified using silica column chromatography (100:10:1 chloroform/methanol/acetic acid).

Ferrocene. We use the previously described procedure[20] to convert ferrocene carboxylic acid to ferrocene succinimidyl ester (Fc-NHS). In brief, we mixed a 5-fold excess of NHS and EDC with ferrocene carboxylic acid in dichloromethane (DCM). The solution was stirred overnight under argon (~12 hr) at room temperature. The resulting solution was then washed with water and the organic phase was collected and dried with $MgSO_4$, filtered, and evaporated. Finally, we used silica column chromatography with diethyl ether to purify the product (Fc-NHS).

Pentamethyferrocene. A suspension of $FeCl_2$ in tetrahydrofuran (THF) was vigorously stirred in the dark 1 hr to produce $FeCl_2$•THF. Separately, n-butyllithium was added drop-wise to pentamethylcyclopentadiene in tetrahydrofuran in a dry ice acetone bath and the mixture was then warmed and stirred at room temperature for 2 hr. We then slowly transferred this mixture into the $FeCl_2$•THF solution and

stirred at room temperature for 1 hr. Sodium cyclopentadienide was slowly added to this via cannula before stirring over night (~16 hr). The resultant pentamethylferrocene product was recrystallized from pentane with a yield of 60%

To obtain pentamethylferrocene carboxylic acid we first mixed 2-chlorobenzoyl chloride and $AlCl_3$ in dichloromethane for 1 hr at 0˚C. We cooled this to -40˚C and then slowly add pentamethylferrocene in dichloromethane. We then warmed the mixture to 15˚C over 60 min to generate 2-chlorobenzoyl-pentamethylferrocene which we then poured onto crushed ice. We next washed the organic phase with 1 M NaOH and dried it against $MgSO_4$ before filtering and evaporating the solvent. We purified the crude 2-chlorobenzoyl-pentamethylferrocene using silica column chromatography (25:1 cyclohexane/methyl tert-butyl ether). We then mixed the 2-chlorobenzoyl-pentamethylferrocene with potassium tert-butoxide and few drops of water in dimethylformamide (DMF) and refluxed the mixture at 110˚C for 1 hr to produce the carboxylic acid. After cooling the mixture to 0˚C we then added 1 M HCl to obtain the red brown solid, which we washed with water, filtered and dried.

To synthesize pentamethyferrocene succinimidyl ester we added NHS and N-(3-dimethylamino-propyl)-N´-ethylcarbodiimidehydrochloride (EDC) to a 25 mM solution of pentamethylferrocene carboxylic acid in dichloromethane to a final concentration of 60 mM each and stirred overnight (~12 hr) under argon at room temperature. The resulting solution was then washed with water and the organic phase was collected and dried with $MgSO_4$, filtered, and evaporated. We then

purified the pentamethyferrocene succinimidyl ester product using silica column chromatography (diethyl ether).

Conjugating the redox reporters to the DNA probes

Conjugation of the redox reporters to the appropriate single-stranded DNA was achieved via the coupling of the NHS-ester redox reporter conjugate with the 5'-alkyl-amino modified single stranded DNA. 10 μL of 200 μM 5'-alkyl-amino DNA was added to 50 μL of a 0.5 M sodium bicarbonate solution (pH 8.5), and 1 μM of the reporter-NHS was dissolved in 10μL dimethyl sulfoxide (DMSO)[20]. We mixed the DNA solution we prepared above and the reporter-NHS DMSO solution, and incubated the mixture for 4 hours in dark at room temperature. After conjugation the DNA was desalted using a spin column (EMP-Biotech) and purified by RP-HPLC (C18 column). The stocked DNA solutions were stored at -20° C for future use. The yield of the final conjugated product, estimate using HPLC and mass spectrometry, was typically about 20% of the DNAs were modified.

Electrode preparation and sensor fabrication

E-DNA sensors were prepared using established procedures[10]. In brief, prior to sensor fabrication, gold disk electrodes (2 mm diameter, CH Instruments, Austin, TX) were cleaned both mechanically (by polishing with diamond and alumina oxide slurries successively) and electrochemically (through successive scans in sulfuric acid solutions) as previously described. The linear probe DNA were reduced for 1 hr at room temperature in 10 mM tris(2-carboxyethyl)phosphine hydrochloride (Molecular Probes, Carlsbad, CA) and then diluted to a final

concentration of 1 μM in 50 mM phosphate /100 mM NaCl buffer, pH 7.0, as was used in all the experiments to follow unless otherwise noted). The gold electrodes were incubated in this solution for 1 hr at room temperature, rinsed with deionized water, and then incubated in 3 mM 6-mercapto-1-hexanol in deionized water for 120 min. After deposition of this molecule onto a gold electrode the electrode surface is "backfilled" with 6-mercapto-1-hexanol to form a continuous, mixed, self-assembled monolayer. Following this, the electrodes were rinsed in deionized water and stored in buffer for future use.

Sensor characterization

Fabricated sensors were interrogated using square wave voltammetry (SWV) with a 50 mV amplitude signal at a frequency of 60 Hz, in the absence and presence of fully complementary target. For the latter measurements the electrodes were incubated for 30 min with the target DNA at 1 μM in 50 mM phosphate, 100 mM NaCl buffer or 20% fetal calf serum in the same buffer. Values with reported error bars represent the average and standard deviations of measurements performed on at least three independently fabricated electrodes. Signal gain was computed by the relative change in SWV peak currents with respect to background current (SWV peak current in the absence of target).

Our sensors were stored in buffer in sealed at room temperature. To test sensor robustness to repeated electrochemical interrogations, sensors were subjected to multiple SWV scans without target using a scan interval in both buffer and 20% serum. To test sensor robustness to multiple testing cycles were assessed by

subjecting the sensors to a repeated cycle of testing, testing in saturating target, and regeneration with a 30 s deionized water rinse. These cycles were repeated 5 times in 20% serum respectively.

2.5 Acknowledgment

This work was supported by the NIH (AI107936) and the Institute for Collaborative Biotechnologies through grant W911NF-09-0001 from the U.S. Army Research Office (KWP). The content of the information does not necessarily reflect the position or the policy of the Government, and no official endorsement should be inferred.

2.5 References

1. Lubin, A.A.; Plaxco, K.W. *Acc. Chem. Res.***2010**, *43*, 496–505.
2. McQuistan, A.; Zaitouna, A.J.; Echeverria, E.; Lai, R.Y.*Chem. Commun.***2014**,*50*, 4690-4692.
3. Boon, E.M.; Salas, J.W.; Barton, J. K. *Nature Biotechnology.***2002**,*20*, 282-286.
4. Fan, C.; Plaxco, K.W.; Heeger, A.J.*Proc. Natl. Acad. Sci. U.S.A.***2003**,100*, 9134-9137.
5. Ikeda, R.; Kitagawa, S.; Chiba, J.; Inouye, M. *Electrode. Chem. Eur. J.***2009**,*15*, 7048–7051.
6. Lubin, A.A.; Lai, R.Y.;Heeger, A.J.; Plaxco, K.W. *Anal. Chem.***2006**, *78*, 5671-5677.
7. Ferapontova, E.E.; Olsen, E.M.; Gothelf, K.V. *J. Am. Chem. Soc.***2008**, *130*, 4256–4258.
8. Mahshid, S.S.; Camiré, S.; Ricci, F.; Vallée-Bélisle, A. *J. Am. Chem. Soc.***2015**, *137*, 15596–15599.
9. Ferguson, B.S.;Hoggarth, D.A.; Maliniak, D.; Ploense, K.; White, R.J.; Woodward, N.; Hsieh, K.; Bonham, A.J.; Eisenstein, M.; Kippin, T.; Plaxco, K.W.; Soh, H.T. *Science Trans. Med*.**2013**, *5*, 213ra165.
10. Xiao, Y.; Lai, R.Y.; Plaxco, K.W. *Nature Prot.* **2007**, *2*, 2875–2880.
11. Rowe, A.A.; Bonham, A.J.; White, R.J.; Zimmer, M.P.; Yadgar, R.J.; Hobza, T.M.; Honea, J.; Ben-Yaacov, I.; Plaxco, K.W. *PLoS One***2011**, *6*, e23783.

12. Kang D.; Xia, F.; Zuo, X.; White, J.R.;Vallée-Bélisle, A.; Plaxco, K.W. *NPG Asia Mat.***2012**, *4*, e1.

13. Xia, J; Daimin Song; Wang, Z.; Zhang, F.; Yang, M.; Gui, R.; Xia, L.; Bi, S.; Xia, Y.; Li, Y.; Xia, L. *Biosensors & Bioelectronics***2015**, *68*, 55-61.

14. Du, Y.; Lim, B.J.; Li, B.; Jiang, Y.S.; Sessler, J.L.; Ellington A.D. *Anal. Chem.***2014**, *86*, 8010–8016.

15. Ren, K.; Wu, J.; Yan, F.; Zhang, Y.; Ju, H. *Biosensors & Bioelectronics***2015**, *66*, 345-349.

16. Gorodetsky, A.A.; Hammond, W.J.; Hill, M.G.;Slowinski, K.; Barton, J.K. *Langmuir***2008**, *24*, 14282-14288.

17. Pheeney, C. G; Barton, J.K. *J. Am. Chem. Soc.***2013**, *135*, 14944–14947.

18. Balintová, J.; Pohl, R.; Horáková, P.; Vidláková, P.; Havran, L.;Fojta, M.;Hocek, M. *Chem. Eur. J.***2011**, *17*, 14063–14073.

19. Zuo, X.; Song, S.; Zhang, J.; Pan, D.; Wang, L.; Fan, C. *J. Am. Chem. Soc.***2007**, *129*, 1042–1043.

20. Kang, D.; Zuo, X.; Yang, R.; Xia, F.; Plaxco, K.W.; White, R.J. *Anal. Chem.***2009**, *81*, 9109-9113.

21. Ricci, F.; Lai, R.Y.; Heeger, A.J.; Plaxco, K.W.; Sumner, J.J. *Langmuir.***2007**, *23*, 6827-6834.

3. Re-engineering electrochemical biosensors to narrow or extend their useful dynamic range[2]

3.1 Abstract

Here we demonstrate two convenient methods to extend and narrow the useful dynamic range of a model electrochemical DNA sensor. We did so by combining DNA probes of different target affinities but with similar specificity on the same electrode. We were able to achieve an extended dynamic response spanning 3 orders of magnitude in target concentration. Using a different strategy we have also narrowed the useful dynamic range of an E-DNA sensor to only an 8-fold range of target concentrations.

[2] This chapter was adapted from a research article published in Angewandte Chemie International Edition. Reproduced in part with permission from [Kang et al. Re-engineering electrochemical biosensors to narrow or extend their useful dynamic range. *Angewandte Chemie International Edition* **2012**, *51*, (27), 6717-6721] Copyright © 2012 WILEY-VCH Verlag GmbH & Co.

3.2 Introduction

The use of electrode-immobilized biomolecules, such as proteins and nucleic acids, represents a common feature among many emerging biotechnologies. For example, the specificity, affinity and versatility of biomolecular recognition has been exploited for the development of a wide range of electrochemical biosensors that show promise for the detection of many clinically and industrially important analytes[1,2]. Such "bioelectronic interfaces" similarly form the basis of biofuel cells[3] and molecular logic gates[4], technologies that have attracted significant recent efforts. Interest in the applications of surface-electrode-bound biomolecular systems is thus rapidly growing.

Despite their often impressive performances, technologies based on biomolecular recognition suffer from the inherent limitation of single-site binding: its fixed dose-response curve characteristics. That is, single-site binding almost invariably produces a fixed, hyperbolic relationship between target concentration and receptor binding (the Langmuir isotherm) for which the useful range (here defined as the range between 10% and 90% site occupancy) spans an 81-fold concentration range[1-4]. This fixed dynamic range reduces the utility of electrochemical biosensors in applications, such as viral load monitoring, in which the concentration of the target molecule can vary over many orders of magnitude. It likewise limits the usefulness of biosensors in applications requiring high sensitivity (a steep relationship between target concentration and output signal), such as in the monitoring of drugs with narrow therapeutic windows. Thus, the possibility to

arbitrarily extend or narrow this fixed dynamic range would prove advantageous in several biosensing applications. Similarly, the ability to extend the dynamic range of biorecognition would likely improve the efficiency of biofuel cells[3], and the ability to narrow the dynamic range would reduce noise in molecular logic gates[4], further illustrating the limitations associated with the fixed dynamic range of most biomolecular recognition.

Recently we have shown that some of the mechanisms employed by nature to alter the otherwise fixed dynamic range of single-site binding can also be used to broaden and narrow the dose-response curves of solution-phase, optical biosensors[5]. For example, by combining together biosensors of identical specificity but differing in affinity we have expanded the useful 81-fold range of a molecular beacon, a model solution-phase optical biosensor, by more than 10,000-fold[5]. In parallel we have also adapted the sequestration mechanism, often employed by nature to generate "ultrasensitive" genetic networks, to narrow the dynamic range of the same biosensor down to 5-fold, thus greatly increasing the sensitivity of this category of biosensors[5].

Following the above work we demonstrate here the application of these approaches to modifying the dynamic range of reagentless, electrochemical biosensors. Specifically, we have used these approaches to arbitrarily narrow and broaden the useful dynamic ranges of electrochemical "E-DNA" sensors[6, 7], a class of conformation-linked DNA platforms that enable the single-step detection of

specific oligonucleotides directly in complex media, such as blood serum and environmental samples (Figure 3-1)[7, 8]

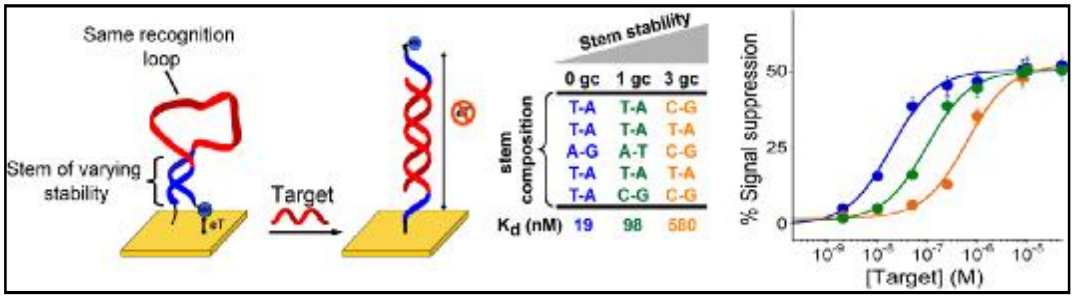

Figure 3-1. (Left) E-DNA sensors consist of a stem-loop DNA modified with a redox reporter (here methylene blue) and attached to an interrogating gold electrode via an introduced thiol group[7]. This probe undergoes a large-scale conformational switch upon hybridization with a DNA complementary to the loop, leading to large change in Faradaic current from the redox reporter. The affinity of such "switch-based" probes can be rationally tuned by many orders of magnitude, without affecting their specificity, by simply altering the stability of their nonbinding, non-signalling state (e.g., by varying the stability of the E-DNA probe's stem with the change of the GC base pairs content)[9]. (Right) Here we have employed a set of three E-DNA probes sharing a common recognition element but spanning almost three orders of magnitude of target affinity. Error bars in this figure and in the following figures represent the average and standard deviations of measurements performed on at least three independently sensors.

3.3 Results and discussion

E-DNA sensors are comprised of a redox-reporter-modified stem-loop DNA-probe (receptor) attached to an interrogating electrode [7]. In the absence of target, the formation of the stem holds the redox reporter into proximity with the electrode, supporting efficient electron transfer. Upon hybridization with a complementary oligonucleotide target, the terminus of the probe is pushed away from the electrode, which, in turn, hinders the efficiency with which electrons are transferred to the electrode and reduces the observed Faradaic current (Figure 3-1). The first strategy we have employed to narrow or extend the dynamic range of this sensor requires the availability of probes directed against the same target molecule but differing in affinity[5]. For the E-DNA sensor this can be achieved by using a set of stem-loop probes that share a common recognition loop, and thus target the same DNA sequence, but differ in the stability of their double-stranded stems. Doing so we can arbitrarily vary the target-probe dissociation constant – here over three orders of magnitude– without affecting the target-recognizing loop, and thus without changing the probe's sequence specificity[5, 9] (Figure 3-1). While the affinity of E-DNA sensors is easily tuned via changes in their stem stability, reaching this objective can be more challenging for structurally less-defined recognition elements. Despite this, a number of rational and semi-rational strategies have been reported by which to engineer (and tune) similar switching mechanisms into aptamers, aptazymes. and even proteins[10]. Loh and co-workers, for example, have recently demonstrated a generic strategy to design novel protein-based switches, termed

"alternate frame folding", in which duplication of a portion of a protein's sequence is used to stabilize an alternative, nonbinding, circularly permuted conformation[10d]. Proteins and nucleic acids can also be engineered to undergo folding-induced conformational changes via the introduction of destabilizing mutations (typically remote from the target binding site so as to ensure that specificity is retained) that push the folding equilibrium toward the nonbinding, unfolded state, thus coupling binding to a conformational change (folding) and simultaneously coupling binding affinity to folding stability[10].

As noted above, traditional E-DNA sensors exhibit a useful dynamic range of 81-fold (Figure 2-1), again defined as the change in concentration required to transition from receptor occupancy of 10% to occupancy of 90%. We can extend this useful dynamic range by co-immobilizing two E-DNA probes differing in affinity for their (common) target DNA onto a single electrode. (Of note, the E-DNA probes we have employed are equally modified with the same methylene blue redox reporter and thus they both signal at the same redox potential and with the same relative signal change at saturating target concentrations, Figure 3-1). To achieve optimal log-linear behavior in the modified sensor, the affinities of the two probes should differ by approximately 30-fold[5]. For example, by combining on the same electrode surface an equimolar concentration of the low-stability 0GC stem-loop probe (Figure 3-1, bottom), which exhibits a dissociation constant of 19 nM, with the more stable 3GC stem-loop probe, exhibiting a dissociation constant of 580 nM, we expand the normally 81-fold dynamic range of this approach to

approximately 1,000 fold (spanning from 2 nM to 2,000 nM) and achieve excellent linearity on a log[concentration] plot (R^2 = 0.978; Figure 3-2).

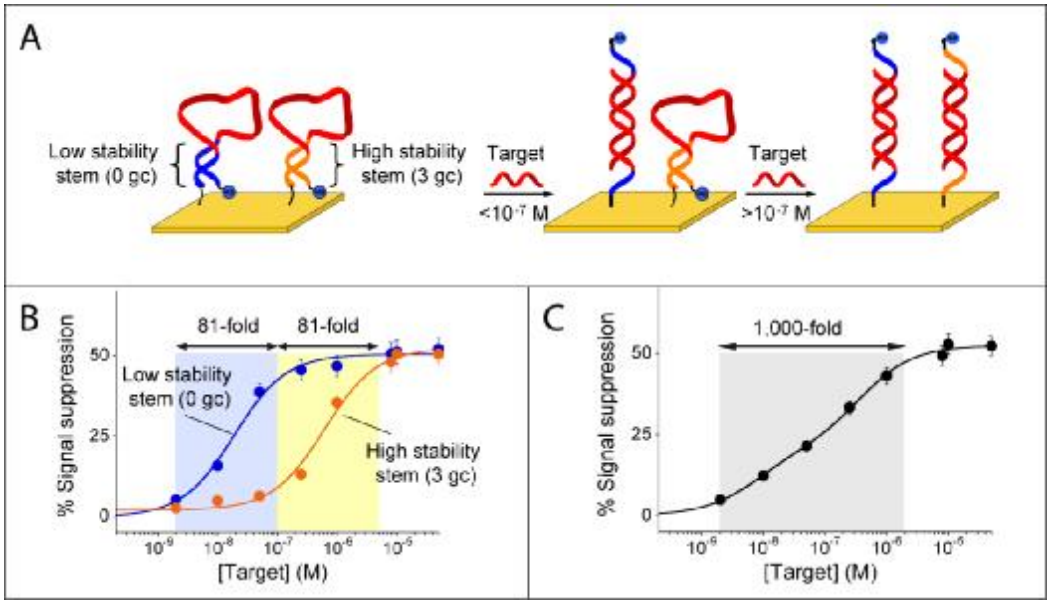

Figure 3-2. Employing a pair of signalling probes differing in affinity we can broaden the dynamic range of E-DNA sensors. (A) We did so by co-immobilizing (1:1 ratio) on a single electrode surface a relatively low affinity E-DNA probe (e.g., probe 3GC, K_d = 580 nM) with a higher affinity E-DNA probe (e.g., probe 0GC, K_d = 19 nM). (B) The useful dynamic range (defined as the fold-concentration change upon transition from 10% occupancy to 90% occupancy) of these individual probes spans an 81-fold range of target concentrations over two distinct concentration regimes. (C) With this strategy the resulting dose-response curve is extended and spans a 1,000-fold range of target concentrations.

The availability of probes retaining a common specificity profile but differing in affinity also provides a means of *narrowing* the useful dynamic range of E-DNA sensors, thus enhancing their sensitivity (the steepness of the input/output curve) and improving their ability to measure small changes in concentration. Specifically, we adapted here the sequestration mechanism used by nature to improve the sensitivity of many regulatory cascades through the competition between a

high-affinity, but not signaling, recognition element (the *depletant*) and a low-affinity signaling receptor [10-12]. To demonstrate this we co-immobilized two E-DNA probes, the stem-loop sequence 1GC and an equivalent, fully linear probe lacking a complementary stem, both of which are complementary to the same 13-base target sequence. Because the linear probe does not undergo a binding-induced conformational change its affinity for the DNA target is significantly greater than that of the stem loop 1GC probe. In this application the higher affinity linear probe lacks any redox reporter (methylene blue) and thus the hybridization of the target to this probe does not produce any measurable signal change. This linear probe therefore acts as the depletant, "silently" sequestering the target until the threshold concentration is surpassed [12]. The lower-affinity signalling probe (1GC) is only activated (and thus only signals the presence of the target) when the depletant is saturated and this threshold is surpassed.

Using this approach we convert the hyperbolic dose-response curve of a traditional E-DNA sensor into an ultrasensitive response with a dynamic range spanning only an 8-fold range of target concentration, an order of magnitude narrower than the dynamic range of a traditional E-DNA sensor (Figure 3-3).

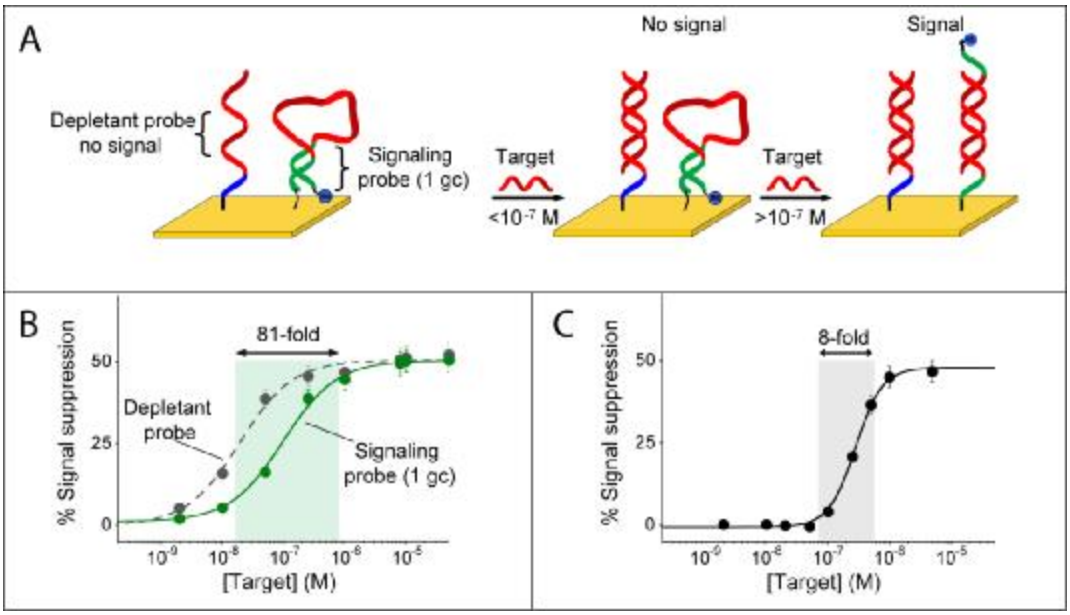

Figure 3-3. Using the sequestration mechanism we can dramatically narrow the useful dynamic range of an E-DNA sensor, thus greatly improving its sensitivity (i.e., its ability to measure small changes in target concentration). (A) We do so by co-immobilizing on a single electrode surface a low affinity, signaling E-DNA probe with a higher affinity probe (depletant) which, lacking the redox reporter, does not signal upon binding its target. At low concentrations the target preferentially binds the depletant, which removes (sequesters) target from the sample without generating a signal. When the total target amount surpasses that of the depletant (the sink is saturated), a threshold response is achieved in which further addition of target dramatically raises the relative concentration of free target. This gives rise to a much steeper dose-response curve than this would occur in the absence of a depletant. (C) Using this approach we have narrowed the 81-fold useful dynamic range of an unmodified E-DNA sensor to a mere 8-fold, thus increasing its sensitivity by an order of magnitude.

The sensitivity achieved via the sequestration mechanism depends on the relative amounts of depletant and signaling probe[12], and thus on the relative density of the two on the sensor's surface. To demonstrate this we have altered the ratio of probe and depletant on our sensors by altering the depletant/probe concentration ratio employed during sensor fabrication [13-15]. To compare sensors fabricated using differing depletant/probe ratios we fitted their input-output curves to the Hill equation, which, although physically meaningful only when used to describe the

ultrasensitivity associated with allosteric cooperativity[16], provides a convenient means of quantifying the steepness of a binding curve. As expected, we observe a "pseudo"-Hill coefficient near unity (1.1±0.1) for sensors lacking the depletant. Upon the addition of the depletant probe, this coefficient increases monotonically with increasing depletant/probe ratios until it plateaus at 2.3 for ratios above 50 (Figure 3-4, right). The highest pseudo-Hill coefficient we have achieved compresses the 81-fold useful dynamic range of an unmodified E-DNA sensor to only 8-fold, significantly increasing the steepness of the dose-response curve of the sensor and, in turn, improving its ability to detect smaller relative changes in target concentration.

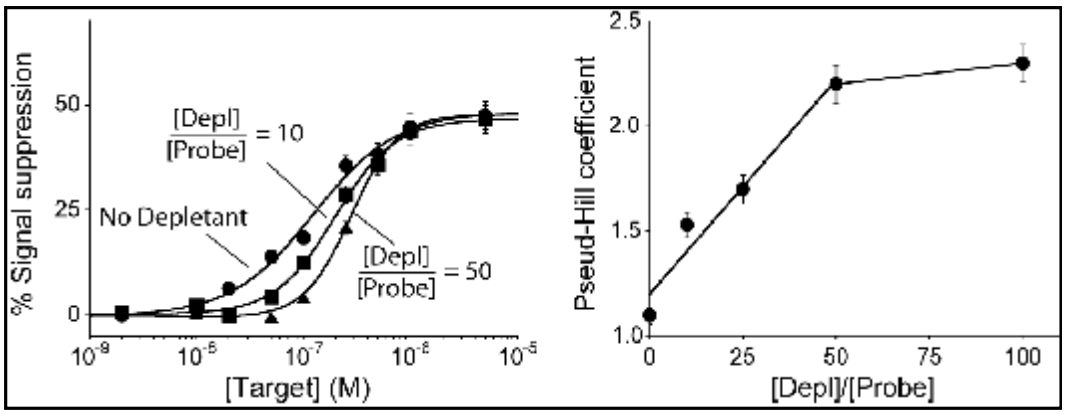

Figure 3-4. The sensitivity (i.e., steepness of the dose-response curve) achieved using the sequestration mechanism depends on the ratio of depletant to probe employed during sensor fabrication. To show this we have fitted our data to obtain pseudo-Hill coefficients, which, although our system is not classically cooperative, are analogous to the Hill coefficient commonly used to describe cooperative enzymatic systems[16]. We find that the pseudo-Hill coefficient increases monotonically with this ratio until plateauing at values above 50.

The above arguments notwithstanding, we must note that this strategy is not without limitations. Specifically, the sequestration approach only works for fixed,

small sample volumes (here we have employed 3 μL samples) so as to avoid the "premature" saturation of the fixed number of depletant molecules on the electrode surface. Moreover, as discussed before, the probe/depletant ratio on surface is a key factor which must be carefully controlled. We did so by assuming that the density ratios on surface are linearly correlated with the concentration ratios deployed in solution during deposition. This (seemingly reasonable) assumption seems confirmed by the linear dependence of the absolute current signals (which are correlated to surface density[14]) versus [probe]/[depletant] ratio (Figure 3-5). However, we note that this correlation could be more complicated for less defined recognition elements which can induce a non-linear immobilization of probe and depletant (Figure 3-6). Finally, the approach proposed is limited to [depletant]/[probe] ratio of 100 over which the signal of the probe is so low that it is not possible to record any significant redox signal (Figure 3-7). Motivated by the above issues, here we also propose the use of an alternative strategy where a fixed concentration of depletant is exogenously added to the mixture solution on each working electrode (Figure 3-8) thus avoiding the problems due to uncontrolled density ratios. Moreover, because the depletant is now free to diffuse in solution, its affinity for the target is greatly increased and this allows to use the same recognition element as both the depletant and the signalling probe, the later being only different from the former due to the presence of the readout tag.

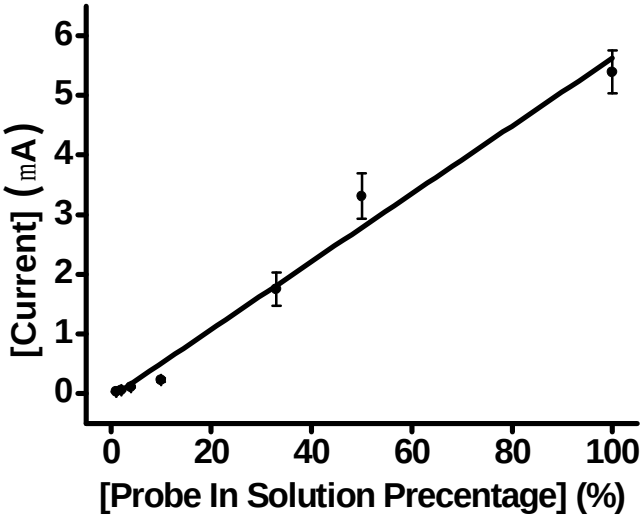

Figure 3-5. Amount of signal probe immobilized on the surface linear response with the percentage of immobilization solution.

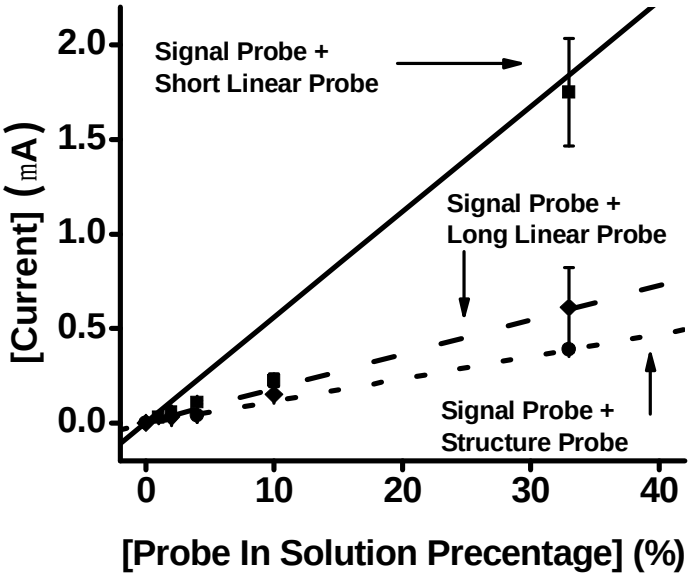

Figure 3-6. Different Probe has different immobilization rate, it is related to the DNA size and structure. The smaller will be faster, and the larger and more complex structure DNA will be slower.

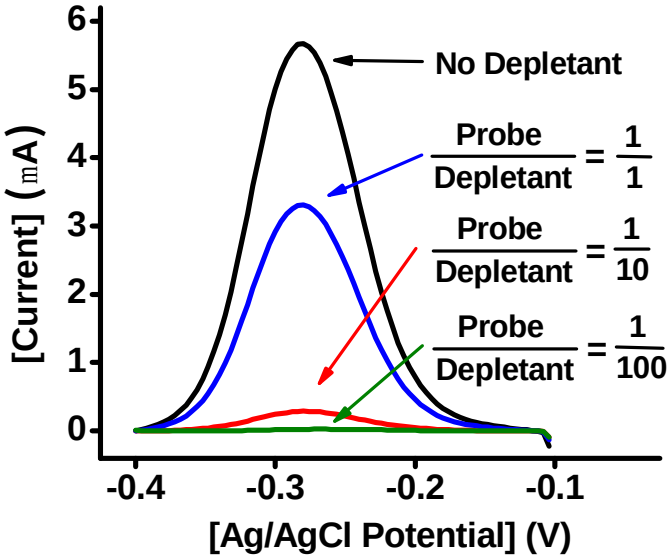

Figure 3-7. Shows four different peak current from different probe: depletant ratio,the approach proposed is limited to depletant/probe ratio of 100 over which signal degradation is so high that it is not possible to record any significant redox signal.

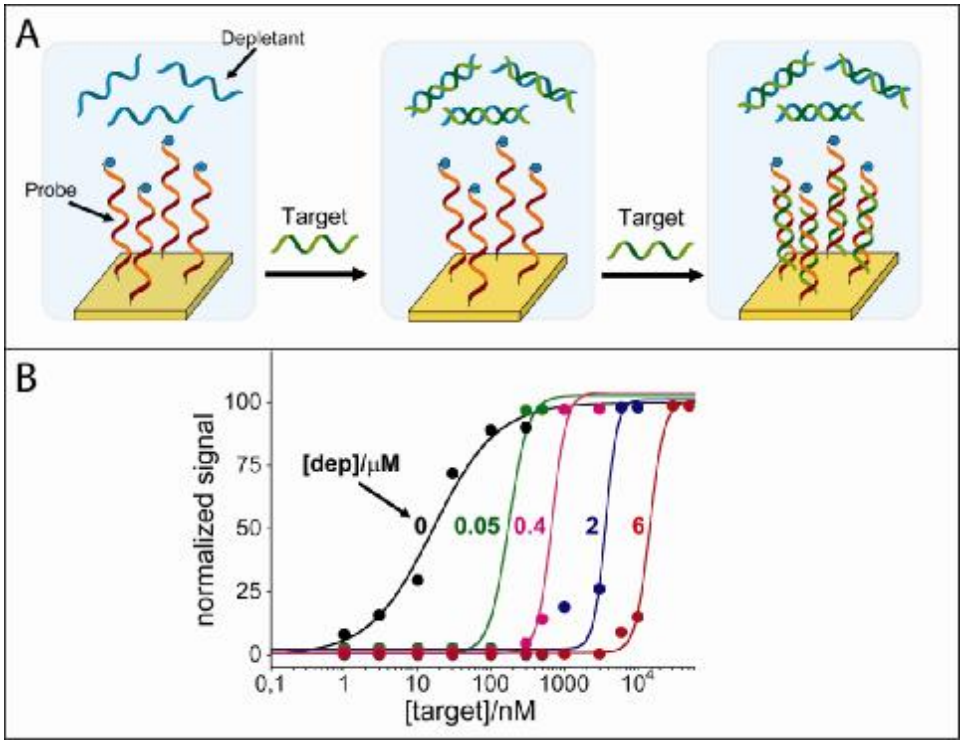

Figure 3-8. To overcome the limitations inherent to the surface attached depletants (which are easily saturated), we also show that the depletant probe can be simply added in solution at a fixed concentration. Here we use an unlabeled non-signalling probe (with the exact same sequence of the signalling redox-labelled probe) that sequesters the target DNA till a threshold level (fixed by the depletant concentration in solution) over which further increase in target concentration results in a steep dose-response curve. Because the depletant is free in solution, it rapidly reacts with the target (and with higher affinity) before this later can diffuse to the electrode surface and "activate" the signalling probe. (B) By using different concentrations of depletant in the reaction mix (0, 0.05, 0.4, 2, 6 M) we can not only achieve steeper transitions than those observed with the depletant co-immobilized with the probe but we can also easily tune the threshold level at which we observe the sharp digital-like response of the sensor.

The unattached "non-signalling" depletant probe sequesters the target DNA until a threshold level (fixed by the depletant concentration) over which further increase in target concentration results in a steep dose-response curve (Figure 3-8). To improve the convenience of this approach a specific amount of depletant has been non-covalently absorbed on the electrode surface and diffuse in solution as soon as the drop solution is applied on the electrode surface, maintaining the single-step

convenience of the fully covalent architectures described above. With this strategy we have built an array of electrodes, each of which containing various concentration of depletant, and thus various target threshold with pseudo-Hill coefficient values between 3 and 4 and a dynamic range spanning only 2-3-fold of target concentration (Figure 3-8),

Here we have demonstrated convenient methods to extend and narrow the useful dynamic range of a model electrochemical DNA sensor. We did so by combining DNA probes of different target affinities but with similar specificity on the same electrode[5]. Employing a pair of signaling probes with dissociation constants differing by approximately an order of magnitude we produced a pseudo-log linear response spanning 3 orders of magnitude in target concentration. And, by employing a pair of probes in which the higher affinity probe is non-signaling we have narrowed the useful dynamic range of an E-DNA sensor to only an 8-fold range of target concentrations, significantly improving its sensitivity. Moreover, because the relevant probes are all strongly chemiadsorbed onto their interrogating electrodes, the modified sensors remain reagentless, reusable, highly selective electrochemical devices readily amenable to lab-on-a-chip applications and point-of-care use[7]. To overcome possible limitations in the application of the strategy employed to narrow the sensor's dynamic range, we have also demonstrated an alternative "sequestration" approach where the depletant does not need to show a higher affinity than the probe itself and is free to diffuse in solution.

Our work is not the first to rationally extend the useful dynamic range of an electrochemical biosensor. Our approach, however, appears rather easier to implement than other, previously reported approaches to this end. This includes approaches based on the use of multiple sensors combined with chemometric strategy[17] or on the use of diffusion barrier membranes[18]. In addition, the use of sets of recognition elements differing only in affinity, and not specificity, represents an advantage over other approaches, such as those utilizing combinations of enzymes differing in both affinity *and* specificity[19], in that it leads to a fixed specificity profile across the sensor's entire dynamic range.

In contrast to broadening the useful dynamic range of electrochemical biosensors, a goal that has seen significant prior literature exploration, we are not aware of any prior literature regarding the narrowing of their dynamic range. The steep dose response curves we achieved open the door to a number of sensing applications requiring high sensitivity and a low signal-to-noise ratio at certain specific target concentration. Of note, compared to a sensor that responds gradually to target inputs, an ultrasensitive electrochemical sensor would be far more useful to generate electrochemical logic gates, ideas that have attracted significant recent interest[20-23].

The approach demonstrated here is general, and can be applied to extend or narrow the dynamic range of other electrochemical biosensors provided that the affinities of the biomolecular recognition elements upon which they are based can be appropriately tuned. This is the case of, for example, conformational-switching

ribozymes and aptamers whose affinity has been rationally modulated through quantitative and predictive model to meet certain performance requirements[24-28]. And despite the rational and semi-rational engineering of proteins or more complex recognition elements is a more challenging task, several examples demonstrate that this is possible and thus potentially rendering our approach to affinity tuning broadly applicable[29-35].

The ability to broaden or narrow the dynamic range of biomolecular recognition could also be of utility in biotechnologies beyond biosensing. The fixed dynamic range of single site binding, for example, limits the utility of biomolecular recognition in biofuel cells, for which wider dynamic range equates to better power efficiencies[36]. It also limits the performance of bio-electronic "logic gates" used in biocomputing, as a steeper, nearly all-or-none "digital" response could significantly reduce the noise floor in such systems [20, 37, 38].

3.3 Experiment and method

Materials and Methods

The following reagents were used as received: sodium phosphate monobasic (Sigma Aldrich), sodium phosphate dibasic heptahydrate (Sigma Aldrich), sodium cloride (Sigma Aldrich), tris(2-carboxyethyl)phosphine hydrochloride (TCEP) (Molecular Probes, Carlsbad, CA).

Signaling probes, depletant probes and target sequences were commercially sourced (Biosearch Technologies, Novato, CA) and used as received. Their sequences were as follows:

Probe 0GC, 5'- HS-$(CH_2)_6$-A TTATT GATCGGCGTTTTA AAGAA G--$(CH_2)_7$-NH-MB-3′

Probe 1GC, 5'- HS-$(CH_2)_6$-A CTATT GATCGGCGTTTTA AATAG G--$(CH_2)_7$-NH-MB-3′

Probe 3GC, 5'- HS-$(CH_2)_6$-A CTCTC GATCGGCGTTTTA GAGAG G--$(CH_2)_7$-NH-MB-3′

Depletant, 5'- HS-$(CH_2)_6$-ATTATT GATCGGCGTTTTA-3′

Target: 5′-TAAAACTCCGATC-3′.

Where -$(CH_2)_7$-NH-MB-3′ represents a methylene blue (MB) added to the terminal phosphate via a C-7 amino linker. Probes and depletant were modified at the 5’ end with a thiol group for attachment to the electrode surface.

Electrode Preparation and Sensor Fabrication

E-DNA sensors were prepared using a well-established previously described procedure [13-15]. In brief, prior to sensor fabrication, gold disk electrodes (2 mm diameter, CH Instruments, Austin, TX) were cleaned both mechanically and electrochemically. Before use, probe and depletant were reduced for 1 hr at room temperature in the dark in 10 mM TCEP. The relevant DNA probes were then immobilized onto freshly cleaned electrodes by incubating for 1 hr in 500 mM NaCl/10 mM potassium phosphate, pH 7 buffer. To achieve a wide dynamic range the probe 0GC and 3GC were mixed in a 1:1 ratio at a total concentration of 1 μM. To narrow the dynamic range of the E-DNA sensors we employed a mixture of probe 1GC and depletant at varying ratios of 1:1, 1:10, 1:25, 1:50 and 1:100 at a total concentration of 1 μM. The electrodes were then rinsed with distilled, deionized water, and incubated in 3 mM 6-mercapto-1-hexanol in 500 mM NaCl/10 mM potassium phosphate, pH 7 buffer for 30 min. Following this, the electrodes were rinsed in water water and stored in buffer for future use.

Electrochemical Measurements

Fabricated sensors were interrogated using square wave voltammetry (SWV) with a 50 mV amplitude signal at a frequency of 60 Hz, before and after a hybridization step with increasing concentrations of the complementary target. To do this, the electrodes were first interrogated in a pure buffer solution (background signal) 1 M NaCl/10 mM potassium phosphate, pH 7 and then incubated for 30 min in a solution

with the appropriate concentration of target DNA. After this incubation, the electrodes were transferred back to the blank buffer solution for a new SWV measurement. Signal gain was computed by the relative change in SWV peak currents with respect to background current. When attempting to achieve a narrow range the volume of the hybridization solution was kept at a minimum allowable of 3 L. In fact, it should be considered that since the depletant is immobilized on the electrode, its amount is fixed and determined by its surface density. The threshold value at which the sensor responds will therefore depend on the volume of the hybridization solution. And since the surface density of a sensor has also a maximal limit, this limits the total amount of depletant available for hybridization with the target and thus could explain the plateau in sensitivity that we observe in our experiments. In addition we note that the ratio of the depletant concentration to the probe concentration employed during sensor fabrication cannot exceed 100; at higher ratios the density of probes on the surface is so low that the electrochemical signal degrades, resulting in unacceptable sensor-to-sensor variability[39]. Values and graphs with reported error bars represent the average and standard deviations of measurements performed on at least three independently fabricated electrodes.

3.4 Acknowledgment

This work was supported by the Italian Ministry of University and Research (MIUR) through the project *FIRB* "*Futuro* in Ricerca" and by NIH through grant AI076899 (Kevin W. Plaxco) .

3.5 Reference

1. Koshland, D.E., *The molecular basis for enzyme regulation.* The enzymes. , ed. P.D. Boyer. Vol. 1. 1970, New York: Academic Press.
2. Goldbeter, A. and D.E. Koshland, *An Amplified Sensitivity Arising from Covalent Modification in Biological-Systems.* Proceedings of the National Academy of Sciences of the United States of America-Biological Sciences, 1981. **78**(11): p. 6840-6844.
3. Koshland, D.E., A. Goldbeter, and J.B. Stock, *Amplification and Adaptation in Regulatory and Sensory Systems.* Science, 1982. **217**(4556): p. 220-225.
4. Ferrell, J.E., *Tripping the switch fantastic: How a protein kinase cascade can convert graded inputs into switch-like outputs.* Trends in Biochemical Sciences, 1996. **21**(12): p. 460-466.
5. Vallee-Belisle, A., F. Ricci, and K.W. Plaxco, *Using Nature's Tricks to Broaden, Narrow and Edit the Dynamic Range of Artificial Biosensors.* Journal of the American Chemical Society, 2011. **in press**.
6. Fan, C.H., K.W. Plaxco, and A.J. Heeger, *Electrochemical interrogation of conformational changes as a reagentless method for the sequence-specific detection of DNA.* Proceedings of the National Academy of Sciences of the United States of America, 2003. **100**(16): p. 9134-9137.
7. Ricci, F. and K.W. Plaxco, *E-DNA sensors for convenient, label-free electrochemical detection of hybridization.* Microchimica Acta, 2008. **163**(3-4): p. 149-155.

8. Lubin, A.A. and K.W. Plaxco, *Folding-Based Electrochemical Biosensors: The Case for Responsive Nucleic Acid Architectures.* Accounts of Chemical Research, 2010. **43**(4): p. 496-505.

9. Vallee-Belisle, A., F. Ricci, and K.W. Plaxco, *Thermodynamic basis for the optimization of binding-induced biomolecular switches and structure-switching biosensors.* Proceedings of the National Academy of Sciences of the United States of America, 2009. **106**(33): p. 13802-13807.

10. Buchler, N.E. and M. Louis, *Molecular Titration and Ultrasensitivity in Regulatory Networks.* Journal of Molecular Biology, 2008. **384**(5): p. 1106-1119.

11. Buchler, N.E. and F.R. Cross, *Protein sequestration generates a flexible ultrasensitive response in a genetic network.* Molecular Systems Biology, 2009. **5**.

12. Ricci, F., A. Vallee-Belisle, and K.W. Plaxco, *High-Precision, In Vitro Validation of the Sequestration Mechanism for Generating Ultrasensitive Dose-Response Curves in Regulatory Networks.* Plos Computational Biology, 2011. **7**(10).

13. Xiao, Y., R.Y. Lai, and K.W. Plaxco, *Preparation of electrode-immobilized, redox-modified oligonucleotides for electrochemical DNA and aptamer-based sensing.* Nature Protocols, 2007. **2**(11): p. 2875-2880.

14. Rowe, A.A., et al., *Fabrication of Electrochemical-DNA Biosensors for the Reagentless Detection of Nucleic Acids, Proteins and Small Molecules.* J Vis

Exp, 2011(52): p. e2922.

15. Kang, D., et al., *Comparing the Properties of Electrochemical-Based DNA Sensors Employing Different Redox Tags.* Analytical Chemistry, 2009. **81**(21): p. 9109-9113.

16. Hill, A.V., *The possible effects of the aggregation of the molecules of haemoglobin on its oxygen dissociation curve.* J. Physiol., 1910. **40**(Suppl.): p. iv-vii.

17. Chow, E., et al., *Extending the dynamic range of electrochemical sensors using multiple modified electrodes.* Analytical and Bioanalytical Chemistry, 2007. **387**(4): p. 1489-1498.

18. Mullen, W.H., et al., *Glucose Enzyme Electrode with Extended Linearity - Application to Undiluted Blood Measurements.* Analytica Chimica Acta, 1986. **183**: p. 59-66.

19. Yamazaki, T., K. Kojima, and K. Sode, *Extended-range glucose sensor employing engineered glucose dehydrogenases.* Analytical Chemistry, 2000. **72**(19): p. 4689-4693.

20. Stojanovic, M.N. and D. Stefanovic, *A deoxyribozyme-based molecular automaton.* Nature Biotechnology, 2003. **21**(9): p. 1069-1074.

21. Saghatelian, A., et al., *DNA-based photonic logic gates: AND, NAND, and INHIBIT.* Journal of the American Chemical Society, 2003. **125**(2): p. 346-347.

22. Adleman, L.M., *Molecular Computation of Solutions to Combinatorial*

Problems. Science, 1994. **266**(5187): p. 1021-1024.

23. Xia, F., et al., *Label-Free, Dual-Analyte Electrochemical Biosensors: A New Class of Molecular-Electronic Logic Gates.* Journal of the American Chemical Society, 2010. **132**(25): p. 8557-+.
24. Hamaguchi, N., A. Ellington, and M. Stanton, *Aptamer beacons for the direct detection of proteins.* Analytical Biochemistry, 2001. **294**(2): p. 126-131.
25. Chen, X. and A.D. Ellington, *Design Principles for Ligand-Sensing, Conformation-Switching Ribozymes.* Plos Computational Biology, 2009. **5**(12).
26. Beisel, C.L. and C.D. Smolke, *Design Principles for Riboswitch Function.* Plos Computational Biology, 2009. **5**(4).
27. Lau, P.S., B.K. Coombes, and Y.F. Li, *A General Approach to the Construction of Structure-Switching Reporters from RNA Aptamers.* Angewandte Chemie-International Edition, 2010. **49**(43): p. 7938-7942.
28. Sefah, K., et al., *Nucleic acid aptamers for biosensors and bio-analytical applications.* Analyst, 2009. **134**(9): p. 1765-1775.
29. Marvin, J.S. and H.W. Hellinga, *Manipulation of ligand binding affinity by exploitation of conformational coupling.* Nature Structural Biology, 2001. **8**(9): p. 795-798.
30. Golynskiy, M.V., et al., *Engineering Protein Switches: Sensors, Regulators, and Spare Parts for Biology and Biotechnology.* Chembiochem, 2011. **12**(3):

p. 353-361.

31. Guntas, G., et al., *Directed evolution of protein switches and their application to the creation of ligand-binding proteins.* Proceedings of the National Academy of Sciences of the United States of America, 2005. **102**(32): p. 11224-11229.

32. Stratton, M.M. and S.N. Loh, *Converting a protein into a switch for biosensing and functional regulation.* Protein Science, 2011. **20**(1): p. 19-29.

33. Strickland, D., et al., *Rationally improving LOV domain-based photoswitches.* Nature Methods, 2010. **7**(8): p. 623-U18.

34. Palmer, A.E., et al., *Ca2+ indicators based on computationally redesigned calmodulin-peptide pairs.* Chemistry & Biology, 2006. **13**(5): p. 521-530.

35. Kohn, J.E. and K.W. Plaxco, *Engineering a signal transduction mechanism for protein-based biosensors.* Proceedings of the National Academy of Sciences of the United States of America, 2005. **102**(31): p. 10841-10845.

36. Bullen, R.A., et al., *Biofuel cells and their development.* Biosensors & Bioelectronics, 2006. **21**(11): p. 2015-2045.

37. Privman, V., et al., *Enzymatic AND-gate based on electrode-immobilized glucose-6-phosphate dehydrogenase: Towards digital biosensors and biochemical logic systems with low noise.* Biosensors & Bioelectronics, 2009. **25**(4): p. 695-701.

38. Wang, J. and E. Katz, *Digital Biosensors with Built-in Logic for Biomedical Applications.* Israel Journal of Chemistry, 2011. **51**(1): p. 141-150.

39. Ricci, F., et al., *Effect of molecular crowding on the response of an electrochemical DNA sensor.* Langmuir, 2007. **23**(12): p. 6827-6834.

4. A new architecture for reagentless, protein-based electrochemical biosensors[3]

4.1 Abstract

Here we demonstrate a new class of reagentless, single-step sensors for monitoring protein-protein and protein-peptide interactions that is the electrochemical analog of fluorescence polarization (fluorescence anisotropy), a versatile optical approach widely employed to this same end. Our electrochemical sensors consist of a redox-reporter-modified protein (the"receptor") site-specifically anchored to an electrode via a short, flexible polypeptide linker. Interaction of the protein with its binding partner alters the efficiency with which the attached reporter approaches the electrode surface, thus changing the observed redox current. As proof-of-principle we employed the bacterial chemotaxis protein CheY as our receptor. Interaction with either of CheY's two binding partners, the P2 domain of the chemotaxis kinase, CheA, or the 16-residue "target region" of the flagellar switch protein, FliM, leads to easily measurable changes in the output voltammetric signal that trace Langmuir-isotherms within error of those seen in solution. Phosphorylation of the surface-bound CheY changes its affinity for both ligands in a manner likewise consistent with the behavior observed in solution. As expected given the proposed sensor signaling mechanism, the signal change observed upon binding depends

[3] This chapter was adapted from a research article in preparation for publication. Reproduced with permission from [Kang et al. A new architecture for reagentless, protein-based electrochemical biosensors]

strongly on the placement of the redox reporter, due presumably to the influence of geometric orientation and steric hindrance. Following these preliminary studies we developed and characterized additional sensors aimed at the detection of specific antibodies (using the relevant antigens as the receptor) that likewise exhibit excellent detection limits without the use of reagents or wash steps. This novel, protein-based electrochemical sensing architecture provides a new and potentially promising approach to quantitative, single-step measurement specific protein-macromolecule interactions.

4.2 Introduction

Among quantitative methods for measuring the levels of specific, diagnostically relevant proteins, only fluorescence polarization (also known as fluorescence anisotropy)[1] has seen widest use in point-of-care application[2-6]. This approach, which reports on the presence of a specific protein-protein complex via binding-induced changes in the tumbling of an attached fluorophore, does not require washing to remove unbound reagents, rendering it one of the more convenient methods for quantifying the levels of specific proteins in clinical samples. Several limitations, however, significantly reduce its utility at the point of care. For example, when challenged with authentic clinical samples the approach requires considerable signal averaging and careful background subtraction. In part this is due to the approach's modest signal gain: the intensity difference between the two polarizations is typically of order ~15% (i.e., 150 millipolarization units) for an antibody-antigen complex, which must be measured against background polarizations typically ranging from 5 to 30% [7-9]. Fluorescence polarization also requires fairly large volumes, necessitating venous blood draws, reducing their utility in point-of-care applications. Finally, the approach is not easily multiplexed, rendering it ill suited for the simultaneous monitoring of, for example, multiple antibodies diagnostic of a single pathogen.

In response to the above arguments a number of groups have developed electrochemistry-based sensing platforms that attempt to capture the generality of fluorescence polarization while avoiding some of its limitations [10-12]. In

previous work, for example, we developed an electrochemical approach utilizing a double-stranded nucleic acid "scaffold" modified on one end to present both a protein-recognizing polypeptide or small molecule and a redox reporter and covalently attached to gold electrode via a flexible linker via the other. The binding of the sensor's target to this recognition element reduces the efficiency with which the attached redox reporter approaches the electrode (analogous to the change in tumbling seen in fluorescence polarization), producing an easily measured change in electron transfer efficiency (analogous to a change in fluorescence polarization) [10, 13-15]. This strategy offers several significant advantages over other methods for detecting protein targets, including the reduced complexity associated with its reagentless, single-step, wash-free format and better performance in complex samples, such as undiluted blood serum and crude soil extracts[10]. Here we expand this promising sensing approach by demonstrating sensors that, rather than using a double-stranded DNA scaffold and a low molecular weight recognition element (e.g., a polypeptide), instead employ full-length proteins as both the recognition element (receptor) and the scaffold, expanding the range of analytes that the approach can target.

4.3 Results and discussion

Here we demonstrate a single-step electrochemical approach for measuring specific protein-protein and protein-peptide interactions that should be expandable to a wide range of other macromolecular targets. As our first test bed we employed as our receptor CheY, a response regulator protein from the *E. coli* chemotaxis signal transduction system. The structure and folding of CheY and its binding to its protein and peptide targets CheA-P2 and $FliM_{16}$ have seen extensive prior study [24-27], rendering them a convenient model system. To convert CheY into a single-step electrochemical sensor we first generated a family of CheY variants containing a carboxy-terminal hexa-his tag with each exposing a single cysteine side chain for conjugation to a maleimide-functionalized methylene blue. To generate our sensors we then used copper complexation with the His-tag to attach each modified protein onto a gold electrode coated with an alkane thiol self-assembled monolayer doped with a small fraction of copper chelating nitrilotriacetic acid (NTA) head groups (Figure 4-1a).

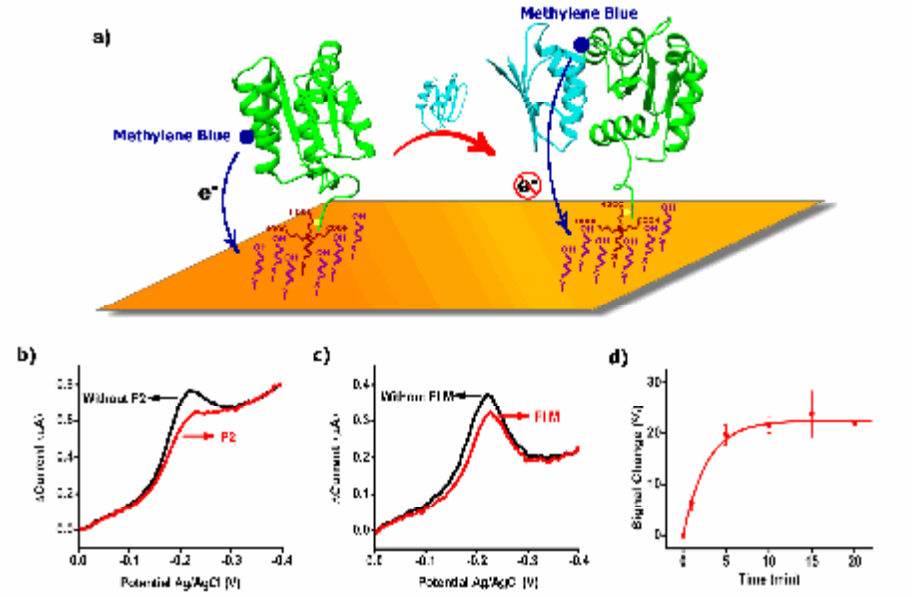

Figure 4-1. Our sensor is comprised of a redox-reporter-modified protein that acts as a recognition element (receptor) attached to a gold electrode via a NTA-modified, thiol-on-gold self-assembled monolayer. **a)** Signal generation occurs when a target protein or peptide binds to this recognition element, reducing the efficiency with which the attached reporter (here methylene blue; shown as a blue dot) transfers electrons to the electrode. **b) & c**) This in turn, leads to an easily measured decrease in faradaic current; shown is the response of a sensor comprised of the bacterial chemotaxis protein CheY with a redox reporter at position 97 to CheY's two naturally occurring binding partners. **d)** The sensor response is rapid; when the CheY-presenting sensor is exposed to 10 μM of the target CheA-P2 it equilibrates with a time constant 2.8±0.7 min^{-1}. The error bars reflect standard deviations of independently fabricated sensors.

Our new sensor architecture responds quantitatively when challenged with the appropriate target molecule. In the absence of either of CheY's binding partners the redox reporter is relatively free to collide with the electrode surface, producing a large faradaic current peak at the redox potential expected for methylene blue (Figure 4- 1a, left) which is reduced in the presence of the protein's binding partners (Figure 4-1a right). For example, for a CheY modified with the redox reporter at position 97, the current falls 22.4 % upon the addition 10 μM of the

ligand CheA-P2, a 74-residue protein that is part of the bacterial chemotaxis system, with a time constant of 2.8±0.7 min^{-1} (Figure 4-1d). The observed signal change increases monotonically with increasing ligand concentration until it approaches saturation at a change of 29% (Figure 4-2). The resultant binding curve is well fitted with Langmuir isotherm module, producing a dissociation constant of 4.5±1.4 μM (Table 4-1), which is within error of the previously reported solution-phase value[28, 29].

Table 4-1. Binding affinities of sensors built with variously placed redox reporters.

Variant	CheY/CheA-P2	CheY-P/CheA-P2	CheY/$FliM_{16}$	CheY-P/$FliM_{16}$
M17C	1.7±0.5 μM	13.5±5.0 μM	10.7±6 μM	0.7±0.25 μM
E37C	5.4 ± 2.7μM	20.3± 6.6 μM	/	/
A71C	4.0 ±1.3 μM	14.7± 5.7 μM	/	/
A80C	5.5±0.2 μM	22.0±13.6 μM	13.2 ± 3.8 μM	0.3±0.07 μM
K97C	4.5±1.4 μM	18.5± 9.2 μM	8.9±4.3 μM	0.25±0.1 μM
E117C	5.5±4.4 μM	28.0±12.0 μM	8.3±2.3 μM	0.5±0.2μM
N121C	2.0±0.5 μM	12.7±3.0 μM	11.5±5.9 μM	1.2±0.4μM

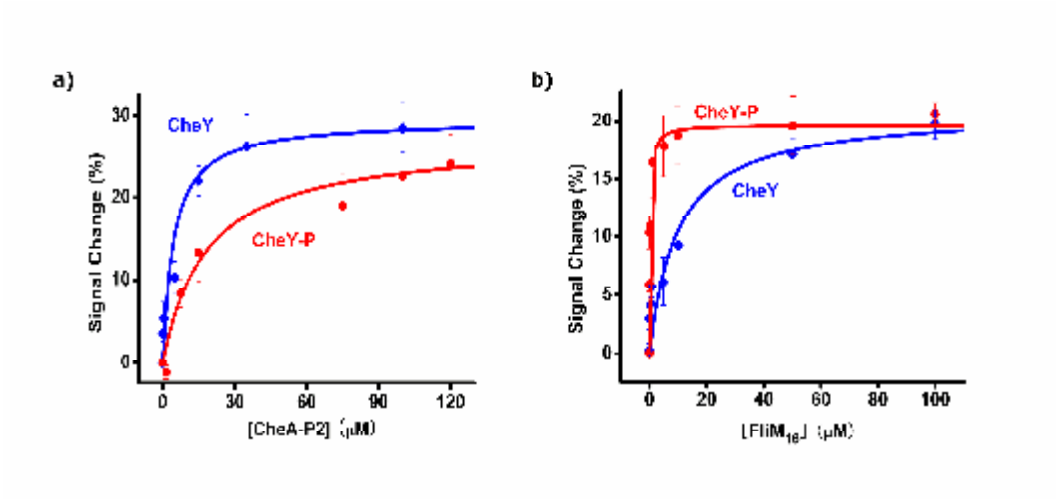

Figure 4-2. Single-step, reagentless detection of the targets **a**) CheA-P2 and **b**) $FliM_{16}$ using CheY modified with methylene blue at residue 97 as the recognition element. As expected based on solution-phase studies, binding affinity is reduced by a factor of 8 for CheA-P2 and a factor of ~35 for $FliM_{16}$ upon CheY phosphorylation. The error bars reflect standard deviations of independently fabricated sensors.

The signal change we observed (peak current change upon the addition of saturating target) depends on both the attachment-position of the methylene blue and the structure of the target. To illustrate the former we fabricated a series of seven sensors differing only in the residue on which the methylene blue was attached using the variants M17C, E37C, A71C, A80C, K97C, E117 and N121C (Figure 4-3). The signal gain observed for these when we employ CheA-P2 as the target range from 9% to 29% (Table 4-2), with the later value larger than the signal change typically seen in fluorescence polarization assays [9]. The largest signal gain occurs when the redox-reporter is placed closest to the P2-binding site (position 97) (Figure 4-2a), suggesting that much of the signal change arises due to steric blocking of the redox reporter by the target protein. Consistent with this, the gain of the sensor is abated when the reporter is positioned farther from the binding site

(e.g., at M17C or N121C). We also investigated the sensor's ability to detect a second naturally occurring binding CheY binding partner, the 16-residue peptide $FliM_{16}$, finding behavior similar to that observed for the detection of P2 (Figure 4-2b; Table 4-2). Specifically, a sensor modified with methylene blue near the binding site (again at residue 97) exhibits the greatest gain (26%). The signal gain observed upon $FliM_{16}$ binding, however, is generally less than that observed upon P2 binding. We presume this occurs as a consequence of the larger bulk of P2, which would more easily hinder approach of the reporter to the electrode.

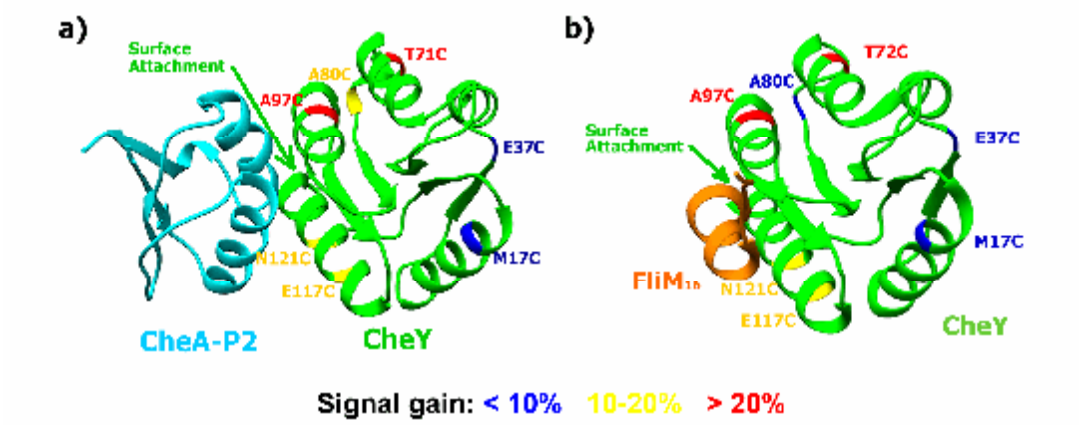

Figure 4-3. The signal gain of our sensors depends on the placement of the redox reporter relative to the target-binding site. Colored residues reflect positions on CheY that we have modified with the methylene blue redox reporter. The coloring indicates the signal decrease seen for each variant upon ligand binding (<10 % blue, 10-20% yellow, >20% red). Not surprisingly, the greatest signal gain is generally observed when the reporter is positioned adjacent to the binding site.

This new sensor architecture is sensitive enough to readily measure the change in binding affinity associated with the phosphorylation of CheY. The phosphorylation of CheY induces allosteric communication between the phosphorylation site (D57) and the protein's target-binding site [23, 26, 30], which in turn facilitates CheY's

dissociation from CheA while strengthening its interactions with the flagellar motor switch protein $FliM_{16}$. Consistent with this, we see significant changes in the binding affinities of surface-bound CheY for both P2 and $FliM_{16}$ upon phosphorylation. Specifically, the phosphorylation of surface-bound CheY reduces the protein's affinity for P2 and enhances its binding to the $FliM_{16}$ (Figure 4-2) in a manner fully consistent with prior solution-phase studies[31, 32]. Finally, mutations known to abolish the activation switch of CheY, such as D57A, show no enhancement of binding as a result of phosphorylation (Table 4-3).

Table 4-2. CheY-P2 and CheY-$FliM_{16}$ binding signal change at different redox reporter locations.

Variant	Signal Change of CheA-P2 Binding	Signal Change of $FliM_{16}$ Binding
M17C	8.6±0.1%	8.5±1.1%
E37C	7.7±2.6%	7.2±0.5%
A71C	26.2±5.2%	25.9±5.3%
A80C	13.0±1.0%	8.9±1.2%
K97C	28.5±3.0%	20.0±1.3%
E117C	15.7±0.5%	14.1±0.9%
N121C	12.1±2.8%	11.1±2.4%

Table 4-3. Binding affinities on D57A deactivated CheY signal change at different position

Deactivated CheY	CheY/$FliM_{16}$	CheY-P/$FliM_{16}$
D57A / M17C	5.4 μM	3.3 μM
D57A / A80C	7.4 μM	4.8 μM
D57A / K97C	3.8 μM	1.1 μM
D57A / E117C	3.5 μM	0.9 μM

Motivated by our success with the use of CheY as a recognition element for the detection of P2 and $FliM_{16}$ we next explored the approach's ability to detect specific antibodies via the inclusion of the relevant antigen as the recognition element. To

do so we first employed green fluorescent protein (GFP) modified with methylene blue at random lysine epsilon amino groups or cysteine thiols as a receptor for the detection of GFP-binding antibodies (Figure 4-4a). Using polyclonal anti-GFP antibodies as our target we observe Langmuir isotherm binding with a dissociation constant 40 ± 8 ng/ml, which is the equivalent of ~0.3 nM for the mixed antibody concentration (Figure 4-4b). As a second test of our ability to detect specific antibodies we employed a disease-related, clinically relevant antigen-antibody pair, the hepatitis B surface antigen (HBsAg) and anti-hepatitis antibodies (HBsAb). Using HBsAg modified with methylene blue at random lysine epsilon amino groups or at cysteine thiols as our recognition element we can detect the antibody with a detection limit of a few nanograms per milliliter (Figure 4-4c), a value that compares well with commercial approaches [33]. A test of this sensor in 20% blood serum, reflecting perhaps more authentic clinical conditions, renders its detection limit effectively unchanged (Figure 4-4d).

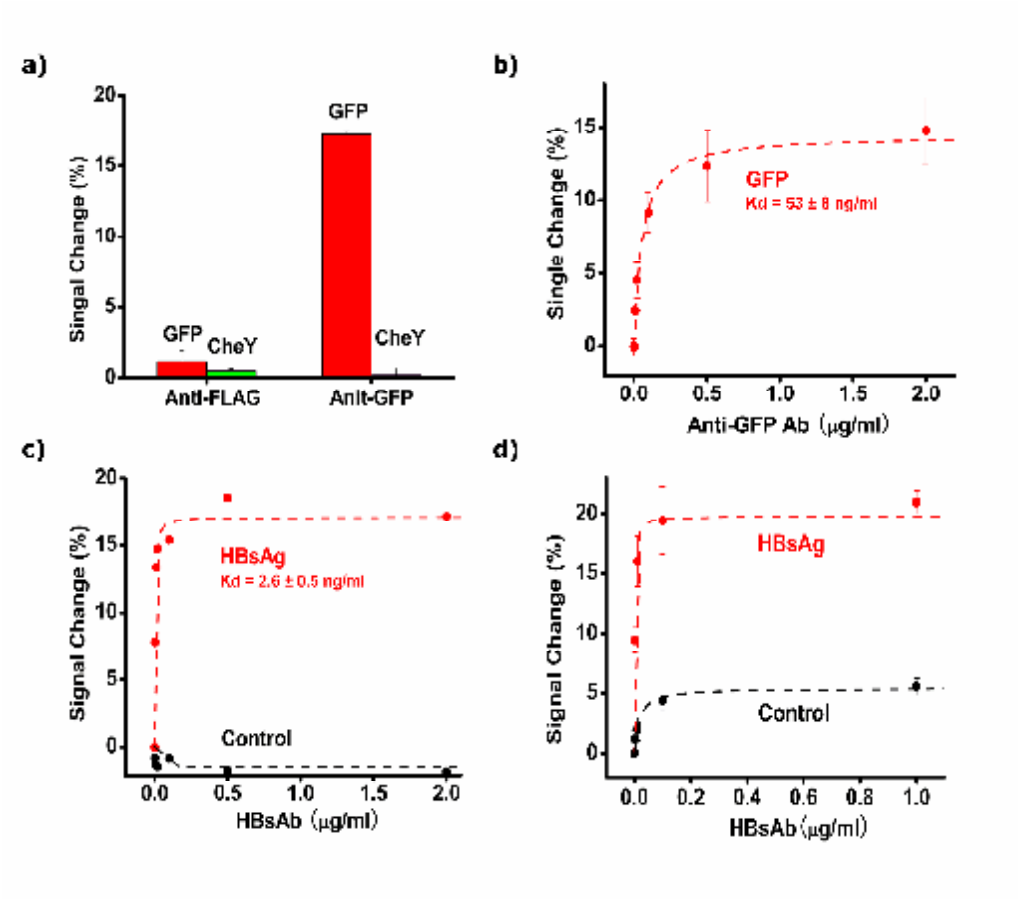

Figure 4-4. The sensing platform can also be used to monitor antigen-antibody interactions. **a**) For example, using an electrode-bound, redox-reporter-modified Green Fluorescent Protein (GFP) as the recognition element we easily detect anti-GFP antibodies at 10 ng/ml (the lowest concentration shown on this plot). In contrast, the sensor does not produce respond to a negative control antibody (anti-FLAG) at 1 μg/ml. Likewise a sensor employing CheY does not produce any signal in response to either anti-Flag or anti-GFP antibodies at 1 μg/ml. **b**) Shown is the monotonic response obtained when the receptor is GFP modified with a methylene blue on random lysine residues. A similar curve is seen for the protein modified on random cysteine residues (Figure 4-5a). **c**) Using a hepatitis B surface antigen (HBsAg) modified with methylene blue on random cysteines as the receptor we can similarly detect antibodies against this protein (HBsAb). A similar curve is seen for the protein modified on random cysteine residues (Figure 4-5b). Shown are binding curves collected in buffer and, **d**), in 20% blood serum. The error bars reflect standard deviations of independently fabricated sensors.

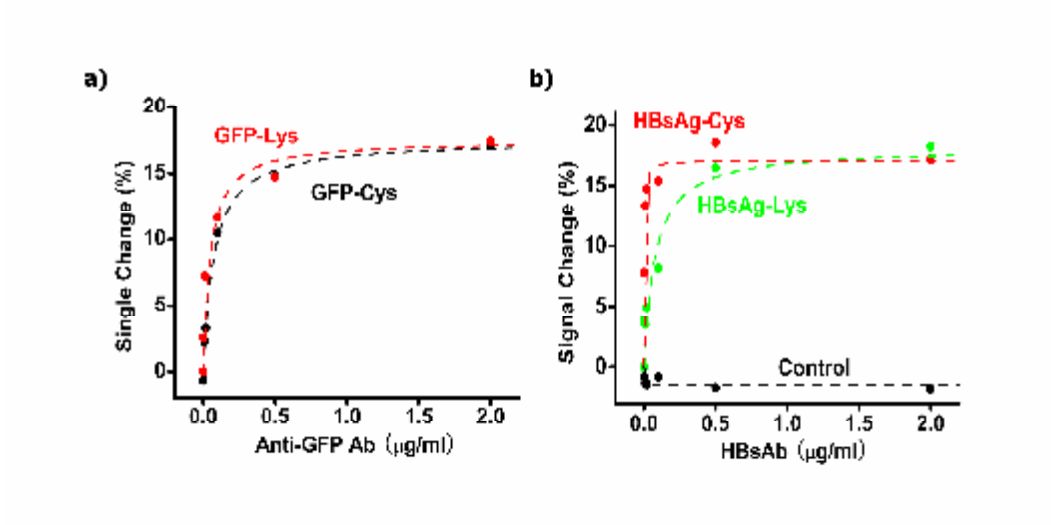

Figure 4-5. Methylene blue was random modified on lysine or cysteine at GFP and HBsAg surface. Both two GFP probes response to Anti-GFP antibody. Compare with the binding we find in HBsAb sensor, the binding curve shapes of lysine random labeling and cysteine random labeling are different.

Here we demonstrate a new class of reagentless, single-step approach to monitoring protein-macromolecular interactions that is the electrochemical analog to optical fluorescence polarization. As proof of principle we have used the approach to monitor the interaction of CheY with its two binding partners, the P2 domain of CheA and the 16-residue peptide $FliM_{16}$ and for the detection of both anti-GFP and anti-HBsAg antibodies. To test the sensitivity of this method for detecting subtle binding affinity changes, we measured the binding affinity switching of CheY between phosphorylated and unphosphorylated states. In all cases we observed binding induced signal changes as large or larger than those typically seen in fluorescence polarization[9] without the need for lights sources, optics, or extensive signal averaging. This new protein-based, electrochemical sensing platform

provides us an alternative means to fluorescence polarization for probing protein-macromolecular interactions and thus may serve as a promising basis for scientific and clinical applications. Similar to fluorescence polarization, for example, our protein based scaffold approach is single step and label-free, rendering it simpler, faster, and, likely, less costly ELISAs and western blots[34]. Beyond this, our approach offers potential advantages over fluorescence polarization, including its relatively inexpensive supporting electronics[35], its ability to perform well in relatively high concentrations of blood serum (Figure 4-4 and Figure 4-6), and the ready multiplexing of electrochemical approaches [36, 37].

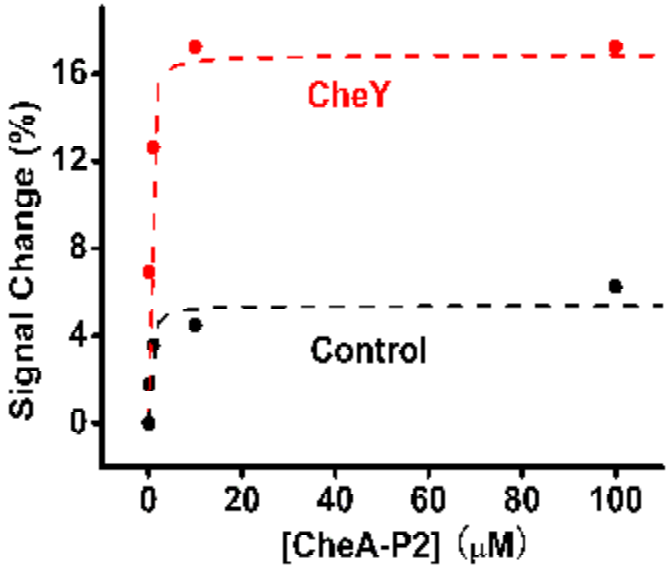

Figure 4-6. We use electrochemical read-out to monitor the binding of surface-attached CheY to the P2 domain of CheA. in 20% serum. Methylene blue was modified at position 97. The maximum signal chang is ~17%. Compare with the same binding curve we got from buffer (28.5%), the signal change in serum is smaller than the change in buffer.

4.3 Experiment and Method

The probe (receptor) proteins were obtained as follows. The gene encoding wild-type *Escherichia coli (E. coli)* CheY (residues 1−129) was cloned into pET28a (Novagen) at the NcoI and XhoI sites in frame with the carboxy-terminal hexahistidine tag. Single-cysteine variants (M17C, E37C, A71C, A80C, K91C, E117C, and N121C) were generated with the QuikChange site-directed mutagenesis kit (Agilent Technologies, Inc.) and transformed into *E. coli* BL21(DE3) (Novagen). The mutagenesis results were checked via sequencing. Transformants were grown at 37°C in lysogeny broth (LB) medium and induced at OD_{600} = 0.4 by the addition of 1 mM isopropyl β-D-1-thiogalactopyranoside (IPTG). The culture was harvested after 3 hr, resuspended in 50 mM sodium phosphate, 10 mM imidazole, 300 mM sodium chloride, pH 8.0 buffer and lysed by French pressure cell press. Cell debris was removed by centrifugation 30000Xg for 30 min before application of the supernatant to an immobilized metal ion (nickel) affinity chromatography column (GE Healthcare). The column was washed with 50 mM sodium phosphate, 300 mM sodium chloride and 35 mM imidazole, pH 8. His-tagged CheY was eluted with 150 mM imidazole in the same buffer, dialyzed into 50 mM sodium phosphate, 150 mM sodium chloride, pH 7.9. The collected fractions were dialyzed and concentrated to ~1 mM. Purity of all variants was >95% as determined by SDS-PAGE electrophoresis. His-tagged green fluorescent protein (GFP) was expressed from pRSET-EmGFP expression plasmid (Invitrogen) in *E. coli* BL21 (DE3) and purified via nickel ion affinity chromatography. The resin was washed with 8 column

volumes of 50 mM sodium phosphate, 300 mM sodium chloride, and 20 mM imidazole, pH 8. Th his-tagged GFP was then eluted with 1 column volume of 250 mM imidazole in the same buffer. GFP containing fractions were dialyzed and concentrated. Purity was >95% as determined by SDS-PAGE electrophoresis. The Hepatitis B virus surface antigen (HBsAg) was purchased from Abcam (Cambridge, MA) without further purification.

The target proteins and peptides were obtained as follows. The CheA P2 domain (residues 156-229) was expressed from the pTM22 plasmid[16] in *E. coli* strain K38 as previously reported[17] and purified by DE52 ion-exchange chromatography (Whatman) and size-exclusion column (Pharmacia). Purity was >95% as determined by SDS-PAGE electrophoresis. The $FliM_{16}$ peptide (MGDSILSQAEIDALLN) was purchased from Macromolecular Resources (Fort Collins, CO) at 90% purity and used without further purification. The anti-GFP polyclonal antibodies and anti-Hepatitis B virus surface antigen polyclonal antibodies (HBsAb) were purchased from Abcam (Cambridge, MA) and used as received.

The maleimide-functionalized methylene blue used as our redox reporter was synthesized starting with 5 mg monocarboxy-methylene blue NHS ester (EMP Biotech) dissolved in 150 µl DMSO. 15 mg N-(2-aminoethyl) maleimide trifluoroacetate salt (Fluka) and 10 µl triethylamine (Sigma-Aldrich) were added followed by 12 hr stirring at room temperature. 50 µl 0.5 M sodium bicarbonate solution was added to this crude reaction mixture and incubated for 2 hr. The final

mixture was dried under reduced pressure and purified using silica column chromatography ($CHCl_3$: methanol 10:1).

The relevant receptor protein was modified with a methylene-blue redox reporter at either cysteine or lysine. For modification at cysteine we employed either single-cysteine variants of CheY or the wild-type cysteines of GFP and HBsAg. These were first reduced by treatment with 5 mM dithiothreitol (Sigma-Aldrich) for 2 hr prior to removal using a Sephadex G-25 spin column (Sigma-Aldrich) immediately followed by the addition of maleimide-modified methlyene blue (as 1-2% v/v solution in DMSO) at a 10:1 reagent-to-protein molar ratio. The reaction mix was incubated at room temperature for 12 hr, and a Sephadex G-25 spin column was then used to remove unreacted methylene blue and exchange the sample into 50 mM sodium phosphate, 150 mM sodium chloride, pH 7.9. For other experiments modified the receptor protein on the epsilon amine group of random lysines. To do so we mixed the wild-type protein with methlyene blue NHS-ester (as 1-2% v/v solution in DMSO) at a 2:1 reagent-to-protein molar ratio in 0.5 M sodium bicarbonate solution (pH 8.5) for 4 hr in dark at room temperature, and then used a Sephadex G-25 spin column to remove unattached methylene blue and exchange the sample into 50 mM sodium phosphate, 150 mM sodium chloride, pH 7.9.

Sensors were prepared by analogy to previously described E-DNA sensors[18, 19]. In brief, prior to sensor fabrication, gold disk electrodes (1.6 mm diameter, CH Instruments, Austin, TX) were cleaned both mechanically (by successively

polishing with 1 m diamond and 0.05 m aluminum oxide slurries) and electrochemically (through successive scans in 0.1M sulfuric acid. 0.01M KCl). Proteins were grafted onto these electrodes using Cu-NTA/His-tag complexation[20, 21] as follows. NTA-thiol (N-[Nα, Nα-bis(carboxymethyl)-L-lysine]-12-mercaptododecanamide, Sigma) was dissolved in methanol at 1 μM concentration. Freshly cleaned electrodes were incubated in this solution for 8 min at room temperature, rinsed with methanol, and then incubated in 3 mM 6-mercapto-1-hexanol in methanol overnight (~16 hr) to form a continuous, mixed, self-assembled monolayer on the gold electrode surface. The NTA-modified electrodes were then rinsed with methanol and incubated with 100 μM copper sulfate in deionized water for 20 min. The electrodes were then incubated with the methylene blue (MB) modified protein for 30 min at room temperature, using 10 μM CheY and GFP or 0.2 mg/ml HBsAg. The electrodes were then washed with 50 mM imidazole in 50 mM sodium phosphate, 500 mM sodium chloride, pH 7.0. The CheY coated electrode was treated with 5 M ultrapure urea (MP Biomedical) in 50 mM sodium phosphate, 100 mM sodium chloride buffer for 10 min in order to remove any non-specifically absorbed protein, rinsed with 50 mM sodium phosphate, 100 mM sodium chloride buffer, and incubated in the buffer for 30 min immediately prior to use (Figure 4-7). The GPF and HBsAg coated electrode were washed with 2% bovine serum albumin (BSA) and 0.05% Tween 20.

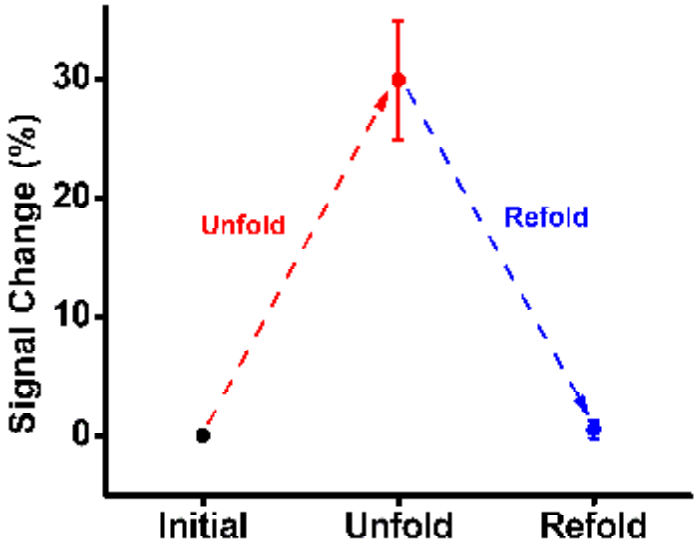

Figure 4-7. When CheY attached on electrode surface, unfold and refolds is reversible under high concentration urea (15 min in 8 M urea, and 30 min after the removal of urea). The refolding yield of the surface-attached protein is quantitative to within experimental error.

Sensors were interrogated using either cyclic voltammetry (CV) with 10 V/s scan rate or square wave voltammetry (SWV) with a 50 mV amplitude signal at a frequency of 100 Hz. Pure sample experiments were performed in 50 mM sodium phosphate, 100 mM NaCl, 20 mM imidazole and serum sample experiments were performed in 50 mM sodium phosphate, 100 mM NaCl with 20% bovine serum. Values with reported error bars represent the average and standard deviations of measurements performed on at least three independently fabricated sensors. Signal gain was computed by the relative change in CV peak or SWV peak currents with respect to background current (CV peak or SWV peak current in the absence of target).

CheY phosphorylation was carried out using 10 mM acetyl phosphate in 50 mM sodium phosphate, 5 mM $MgCl_2$, 100 mM NaCl. The freshly prepared CheY electrodes were incubated in 10mM acetyl phosphate in buffer for 30 min before test. CheY was phosphorylated by acetyl phosphate on the surface[22, 23] immediately prior to measuring binding.

4.4 Acknowledgment

This work was supported by the NIH (R01AI107936) (Kevin W. Plaxco) and NIH (R01GM59544) (Frederick W. Dahlquist)

4.5 Reference

1. Dandliker, W.B., et al., *Fluorescence Polarization Immunoassay - Theory and Experimental Method.* Immunochemistry, 1973. **10**(4): p. 219-227.
2. Melanson, S.E.F., *Implementing Drug-of-Abuse Testing at the Point of Care: Device Characteristics and Decision Criteria With Selected Emphasis on the Biosite Triage System.* Point of Care, 2005. **4**(3): p. 123-127.
3. von Lode, P., *Point-of-care immunotesting: Approaching the analytical performance of central laboratory methods.* Clinical Biochemistry, 2005. **38**(7): p. 591-606.
4. Jameson, D.M. and J.A. Ross, *Fluorescence Polarization/Anisotropy in Diagnostics and Imaging.* Chemical Reviews, 2010. **110**(5): p. 2685-2708.
5. Lea, W.A. and A. Simeonov, *Fluorescence polarization assays in small molecule screening.* Expert Opinion on Drug Discovery, 2011. **6**(1): p. 17-32.
6. Nguyen, H.H., et al., *Surface Plasmon Resonance: A Versatile Technique for Biosensor Applications.* Sensors, 2015. **15**(5): p. 10481-10510.
7. Nielsen, K. and D. Gall, *Fluorescence polarization assay for the diagnosis of brucellosis: A review.* Journal of Immunoassay & Immunochemistry, 2001. **22**(3): p. 183-201.
8. Lucero, N.E., et al., *Fluorescence polarization assay for diagnosis of human brucellosis.* Journal of Medical Microbiology, 2003. **52**(10): p. 883-887.
9. Rossi, A.M. and C.W. Taylor, *Analysis of protein-ligand interactions by*

fluorescence polarization. Nature Protocols, 2011. **6**(3).

10. Cash, K.J., F. Ricci, and K.W. Plaxco, *An Electrochemical Sensor for the Detection of Protein-Small Molecule Interactions Directly in Serum and Other Complex Matrices.* Journal of the American Chemical Society, 2009. **131**(20): p. 6955-+.
11. Gerasimov, J.Y. and R.Y. Lai, *An electrochemical peptide-based biosensing platform for HIV detection.* Chemical Communications, 2010. **46**(3): p. 395-397.
12. McQuistan, A., et al., *Use of thiolated oligonucleotides as anti-fouling diluents in electrochemical peptide-based sensors.* Chemical Communications, 2014. **50**(36): p. 4690-4692.
13. Cash, K.J., F. Ricci, and K.W. Plaxco, *A general electrochemical method for label-free screening of protein-small molecule interactions.* Chemical Communications, 2009(41): p. 6222-6224.
14. White, R.J., et al., *Wash-free, Electrochemical Platform for the Quantitative, Multiplexed Detection of Specific Antibodies.* Analytical Chemistry, 2012. **84**(2): p. 1098-1103.
15. Bonham, A.J., et al., *Detection of IP-10 protein marker in undiluted blood serum via an electrochemical E-DNA scaffold sensor.* Analyst, 2013. **138**(19): p. 5580-5583.
16. Morrison, T.B. and J.S. Parkinson, *Liberation of an Interaction Domain from the Phosphotransfer Region of Chea, a Signaling Kinase of*

Escherichia-Coli. Proceedings of the National Academy of Sciences of the United States of America, 1994. **91**(12): p. 5485-5489.

17. Mcevoy, M.M., et al., *Nuclear-Magnetic-Resonance Assignments and Global Fold of a Chey-Binding Domain in Chea, the Chemotaxis-Specific Kinase of Escherichia-Coli.* Biochemistry, 1995. **34**(42): p. 13871-13880.
18. Xiao, Y., A.A. Rowe, and K.W. Plaxco, *Electrochemical detection of parts-per-billion lead via an electrode-bound DNAzyme assembly.* Journal of the American Chemical Society, 2007. **129**(2): p. 262-263.
19. Rowe, A.A., et al., *Fabrication of Electrochemical-DNA Biosensors for the Reagentless Detection of Nucleic Acids, Proteins and Small Molecules.* Jove-Journal of Visualized Experiments, 2011(52).
20. Hochuli, E., H. Dobeli, and A. Schacher, *New Metal Chelate Adsorbent Selective for Proteins and Peptides Containing Neighboring Histidine-Residues.* Journal of Chromatography, 1987. **411**: p. 177-184.
21. Sigal, G.B., et al., *A self-assembled monolayer for the binding and study of histidine tagged proteins by surface plasmon resonance.* Analytical Chemistry, 1996. **68**(3): p. 490-497.
22. Lukat, G.S., et al., *Phosphorylation of Bacterial Response Regulator Proteins by Low-Molecular-Weight Phospho-Donors.* Proceedings of the National Academy of Sciences of the United States of America, 1992. **89**(2): p. 718-722.
23. Appleby, J.L. and R.B. Bourret, *Proposed signal transduction role for*

conserved CheY residue Thr87, a member of the response regulator active-site quintet. Journal of Bacteriology, 1998. **180**(14): p. 3563-3569.

24. Schuster, M., R.E. Silversmith, and R.B. Bourret, *Conformational coupling in the chemotaxis response regulator CheY.* Proceedings of the National Academy of Sciences of the United States of America, 2001. **98**(11): p. 6003-6008.

25. Baker, M.D., P.M. Wolanin, and J.B. Stock, *Signal transduction in bacterial chemotaxis.* Bioessays, 2006. **28**(1): p. 9-22.

26. Dyer, C.M. and F.W. Dahlquist, *Switched or not?: the structure of unphosphorylated CheY bound to the N terminus of FliM.* Journal of Bacteriology, 2006. **188**(21): p. 7354-7363.

27. Mo, G.Y., et al., *Solution Structure of a Complex of the Histidine Autokinase CheA with Its Substrate CheY.* Biochemistry, 2012. **51**(18): p. 3786-3798.

28. Li, J.Y., et al., *The Response Regulators Cheb and Chey Exhibit Competitive-Binding to the Kinase Chea.* Biochemistry, 1995. **34**(45): p. 14626-14636.

29. Swanson, R.V., et al., *Localized Perturbations in Chey Structure Monitored by Nmr Identify a Chea Binding Interface.* Nature Structural Biology, 1995. **2**(10): p. 906-910.

30. Zhao, R., et al., *Structure and catalytic mechanism of the E. coli chemotaxis phosphatase CheZ.* Nat Struct Mol Biol, 2002. **9**(8): p. 570-575.

31. Welch, M., et al., *Phosphorylation-Dependent Binding of a Signal Molecule*

to the Flagellar Switch of Bacteria. Proceedings of the National Academy of Sciences of the United States of America, 1993. **90**(19): p. 8787-8791.

32. Shukla, D. and P. Matsumura, *Mutations Leading to Altered Chea Binding Cluster on a Face of Chey.* Journal of Biological Chemistry, 1995. **270**(41): p. 24414-24419.

33. Tsai, H.Y., et al., *Determination of hepatitis B surface antigen using magnetic immunoassays in a thin channel.* Biosensors & Bioelectronics, 2010. **25**(12): p. 2701-2705.

34. Crowther, J.R.W., J. M., *The ELISA Guidebook.* Vol. 104. 2001, Totowa, New Jersey: Humana Press Inc.

35. Rowe, A.A., et al., *CheapStat: An Open-Source, "Do-It-Yourself" Potentiostat for Analytical and Educational Applications.* Plos One, 2011. **6**(9).

36. Kang, D., et al., *DNA biomolecular-electronic encoder and decoder devices constructed by multiplex biosensors.* Npg Asia Materials, 2012. **4**.

37. Xia, J.F., et al., *Single electrode biosensor for simultaneous determination of interferon gamma and lysozyme.* Biosensors & Bioelectronics, 2015. **68**: p. 55-61.

5. Study of the force profiles of short single and double-stranded DNAs on a gold surface using a surface forces apparatus[4]

5.1 Abstract

Using a surface forces apparatus (SFA) we have studied the conformation changes of 25-base single and double-stranded DNAs immobilized on gold surface. Our results confirm the previously proposed "mushroom-like" structure of surface-attached single-stranded DNA. Upon the addition of complementary DNA we observe a clear transition from single to double stranded DNA, with the latter exhibiting a rigid rod structure. The formation of double-stranded DNA significantly increases the SFA-observed thickness of the DNA monolayer and the range of repulsion force measured. Our study provides insights into the structure of surface-attached short chain DNAs, which is critical to the design and optimization of DNA based microarrays and sensors.

[4] This chapter was adapted from a research article in preparation for publication. Reproduced with permission from [Kang et al. Study of the force profiles of short single and double-stranded DNAs on a gold surface using a surface forces apparatus]

5.2 Introduction

Biomolecules grafted onto artificial surfaces play increasingly important roles in a range of biotechnologies. DNA-based sensors and sensor arrays, for example, are increasingly widely used in on-chip assays with applications that span broadly across the fields of biology and biomedicine, including gene sequencing, expression screening, drug discovery, and biosensing [1-8].

Despite their importance to many emerging technologies, our understanding of the physics of surface-bound DNAs remains in its infancy[9]. For example, while studies of long DNAs have shown that the behavior of surface tethered DNA follows the same physics as surface attached polyelectrolytes[10-12], the DNA "probes" used in DNA microarrays and DNA-based sensors are typically only few tens of bases or base-pairs long [2]. The short chain length, long persistence length (~ 1nm for single stranded DNA and 50 nm for double stranded DNA), and complex structures (hybridization and secondary structure) often cause the breakdown of polyelectrolyte scaling theory.[12]To our best knowledge, there are only very a few studies that directly address the shorter DNA immobilization and interactions between DNA molecules and surfaces[12-14]. Neither is an accurate model that describes the behavior of short length DNA grafted on surface. In practical, our E-DNA platform typically use short piece DNA from 15 bases to 50 bases length, our results have seen moderate DNA coverage leading to higher signal suppression of our E-DNA sensor. The signal suppression decreases monotonically with decreasing probe density until leveling off at a mean probe separation. But the

physical mechanisms still have not been deeply studied. To understand how the DNA behaved on surface will help us to design our sensor to achieve better performance.

The characterization of the structure of surface tethered DNA remains challenging due to the complex inter-molecular interactions and DNA surface interactions. Several techniques have been used to study surface grafted DNA, including atomic force microscopy (AFM)[15-17], X-ray photoelectron spectroscopy (XPS)[14], Fourier transform infrared (FTIR) spectroscopy[18], near-edge X-Ray absorption fine structure (NEXAFS)[19], surface plasma resonance (SPR)[20], electrochemistry[21-23] and fluorescence microscope[10]. To gain a more comprehensive understanding of single-stranded DNA immobilized onto a surface, it is important to develop an approach that provides quantitative characterization, while also allowing direct comparison between different conditions (for example, with different immobilization densities, hybridization condition and ionic strength).

Here we introduce the surface force apparatus (SFA) technique to characterize the structure of immobilized single-stranded DNA on a gold surface. The SFA is a powerful technique to study the structure and interactions of surface tethered polymers. The SFA can provide direct information on the structure of DNA within the monolayer and make in-situ hybridization measurement. Our force measurements reveal the changes on DNA chain conformation and flexibility before and after the hybridization.

5.3 Result and discussion

Using a surface forces apparatus, we measured the repulsive force of compressing a 25-base single-stranded DNA monolayer grafted on a gold surface to a bare mica surface. The ionic strength of our buffer solution is 0.6 M, which gives a Debye length of $1/\kappa = 0.4$ nm. Under such conditions, the electrostatic interactions are largely screened out, and the entropic steric repulsion and DNA chain elasticity dominate the measured force. The normal force was measured when compressing the grafted single-stranded DNA layer against a bare mica surface as a function of distance between two opposing surfaces (Figure 5-1a). The measured force distance profile shows a hard wall distance of about 2 nm at a compression of 10 mN/m, and a single exponential decay with a decay length of 1.3 nm.

We then sequentially hybridized the surface tethered single-stranded DNA chains by immersing the surface into solutions containing different concentrations (50aM, 500aM, 1pM, and 50 pM) of 25-base complementary DNA chains, which will hybridize with the grafted single-stranded DNA (Figure 5-1a).When plotting the force-distance profiles measured by the SFA in a semi-log plot, the force profiles show a clear conformation change of the surface tethered DNA before and after hybridization (Figure 5-1b). The range of repulsion and film thickness gradually increases with degree of DNA hybridization. For all the measurements with different degrees of hybridization, the repulsion forces measured start at the same distance (~ 15 nm). This distance is longer than the contour length of the DNA chains used in this study (~ 10 nm). This is due to a charge regulation effect in

dynamic force measurements, and has been observed in other strong charged systems.[13, 26] At about 10 nm, the repulsion increases more rapidly due to the steric repulsion of the double-stranded DNA chains. Beyond 10 nm, the force profiles all show a linear trend. The slope of the force profiles gradually increases with degree of DNA hybridization.

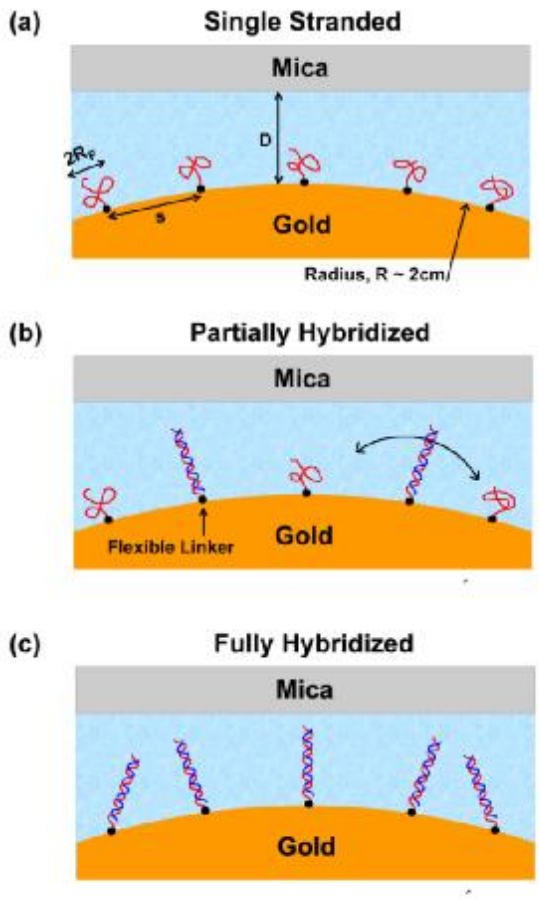

Figure 5-1. The experimental setup used in this study.Using SFA, we measured the interactions between a gold surface grafted with a monolayer of DNA oligomers and a bare mica surface as a function of the distance between two surfaces with three different DNA hybridization states: (a) single-stranded DNA oligomers, (b) partially hybridized DNA oligomers, and (c) fully hybridized DNA oligomers.The mica surface moves towards and away from gold surface in the force measurements.

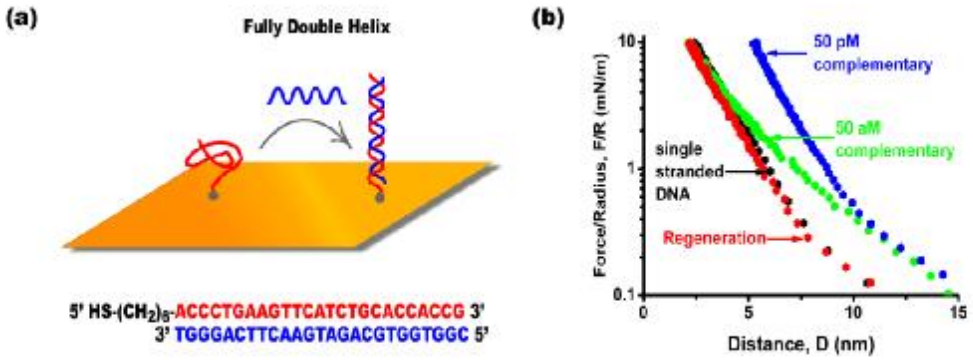

Figure 5-2. (a) One 25-base complementary DNA oligomer in solution hybridizes with a 25 bases DNA oligomer grafted on the gold surface, forming a full double helix. (b) During the sequential hybridization, the range of repulsion gradually shifts out from 10 nm to 15 nm.

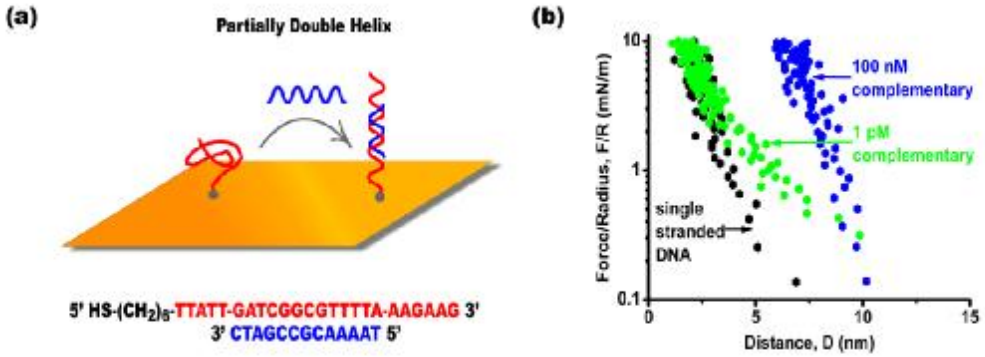

Figure 5-3. (a) One13-base complementary DNA oligomer in solution hybridizes with a25-base DNA oligomer grafted on the gold surface, forming a partial double helix. (b) Normal force profile of a monolayer of single-stranded DNA grafted to a gold surface compressing against a bare mica surface shows a single exponential decay. The range of repulsion gradually shifts out in the sequential hybridization experiment.

To further investigate the effect of hybridization to the structure of surface tethered DNA oligomers, we designed a new 25-base single-stranded DNA sequence, ACCCTGAAGTTCATCTGCACCACCG and its full-length complementary DNA

sequence, and performed a new titration experiment. We then sequentially hybridized the surface tethered single-stranded DNA chains by immersing the surface into solutions containing different concentrations (1 pM, 10 pM, 1nM, and 100 nM) of 13-base complementary DNA chains, which will hybridize with the 13 center bases of the grafted single-stranded DNA (Figure 5-2a). Hybridization significantly changes the conformation of the grafted DNA oligomers, leading to longer ranged repulsions and larger film thicknesses measured by the SFA.

To study the density effect of surface tethered DNA, we apply two differents DNA surface coverage (Figure 5-4). The low density surface we seen the force profile has a linear relationship in semi-log plot, the force kicked in form ~10 nm and increase with the press to ~2 nm. The high density surface force profile is significant different to the low density one. We not only seen the force kicked in much earlier and the slop after the distance smaller than ~10 nm become steeper. And the hard wall shift ~ 4 nm under the same pressure. When we hybridize the low density surface, the force curve shifted 3~4 nm. But there is no significant change when we hybridize the high density surface (Figure 5-5).

Effect of hybridization. Increasing the length of the complementary DNA from 13-base to 25 base leads to two significant differences in the force-distance profiles of the fully hybridized DNA monolayer:(1) the repulsion further extends to a larger separation distance, starting when two surfaces are 15 nm apart (Figure 5-4), and (2) effect of hybridization can be measured at much lower complementary DNA

concentration. Both of the differences are due to the longer complementary DNA chain. The fully hybridized, double-stranded DNA is much more rigid than surface tethered single-stranded DNA. Since the contour length of our double-stranded DNA chains (~10 nm) is much shorter than the persistence length of double-stranded DNA (~ 50 nm), they act like rigid rods but are free to rotate and tilt at the anchoring ends due to the flexible linker between the thiol-gold bond and the DNA chain (Figure 5-1b), leading to a longer range repulsion. Doubling the length of the complementary DNA also favors the hybridization process. According to the equilibrium dissociation constant relationship to Gibbs free energy, we have an equation:

$$\Delta G = -RT\ln K_d \quad (1)$$

Where K_d is the equilibrium constant for the dissociation of the double-stranded DNA.

The calculated binding free energy of the hybridized DNA sequences correlates well with the minimum concentration of the complementary DNA required to cause a significant difference in the repulsion measured by the SFA. The binding free energy of the 13-base complementary DNA sequenceis-18 kcal/mol, as calculated by the M-fold software[27]. The binding free energy yields an equilibrium dissociation constant K_d of 10^{-13} M. Our SFA results show a significant shift of the force curve at 1 pM complementary DNA concentration, which matches the calculated result (Figure 5-3b). For the 25-base complementary DNA samples, the calculated binding free energy ΔG is -38.5 kcal/mol, which yields an equilibrium

dissociation constant of K_d ~10^{-28} M. In comparison to the calculation, surface force measurements only show a noticeable change with attomole level concentration of complementary DNA in solution. In this situation, the hybridization process becomes a diffusion-limited process and the process is out of equilibrium. Nevertheless, the conformation change of surface tethered DNA with attomole level complementary DNA in solution can still be clearly revealed by the SFA measurements, which is very challenge for other characterization techniques.

Effect of grafting density. The grafting density strongly affects the structure and hybridization process of the single-stranded DNA monolayer. Increasing the grafting density σ from ~0.01 chain/nm^2 to ~0.1 chain/nm^2 gives rise to larger monolayer thickness and higher repulsion force (Figure 5-4a). This could be explained by a classic "mushroom" to "brush" transition of surface tethered single-stranded DNA occurring at high grafting density, where neighboring strands interact with one another causing them to extend away from the surface (Figure 5-4b). At a low grafting density, the neighboring single-stranded DNA chains do not overlap each other laterally, forming a so-called mushroom configuration. The free energy of the single-stranded DNA chains in the mushroom regime confined between two planar surfaces can be approximated by an exponential repulsive potential:

$$\mathrm{E(D)} = 36\Gamma \mathrm{kTe}^{-\mathrm{D}/\mathrm{R_F}} \ , \qquad (2)$$

Where $\Gamma = s^2$ is the density of the DNA chains in units of molecular per square meter and R_F is the Flory radius of the single-stranded DNA chains. In the SFA

geometry, equation (2) can be rewritten as

$$\frac{F(D)}{R} = 2\pi E(D) = 72\pi\Gamma kTe^{-D/R_F} \qquad (3)$$

Fitting the forces-distance profiles of the single-stranded DNA monolayers measured at low density. We obtained s_1= 6.9 nm, R_F = 1.5 nm for the low density DNA monolayer.

When the grafting density becomes higher, the neighboring single-stranded DNA chains start overlaps each other laterally. When the distance s between each molecule is smaller than R_F, the single stranded DNAs form brush configuration. We apply the brush fitting:

$$\frac{F(D)}{R} = 2\pi E(D) = 32\pi\Gamma^{3/2}kTe^{-\pi D/L} \qquad (4)$$

and s_2= 0.9 nm, L = 7.1 nm for the high density DNA monolayer.

The fitting results confirms that the low density single-stranded DNA monolayer is in the mushroom regime as $s_1 > R_F$, and the high density single-stranded DNA monolayer is in the brush regime ($s_2 < R_F < L$).

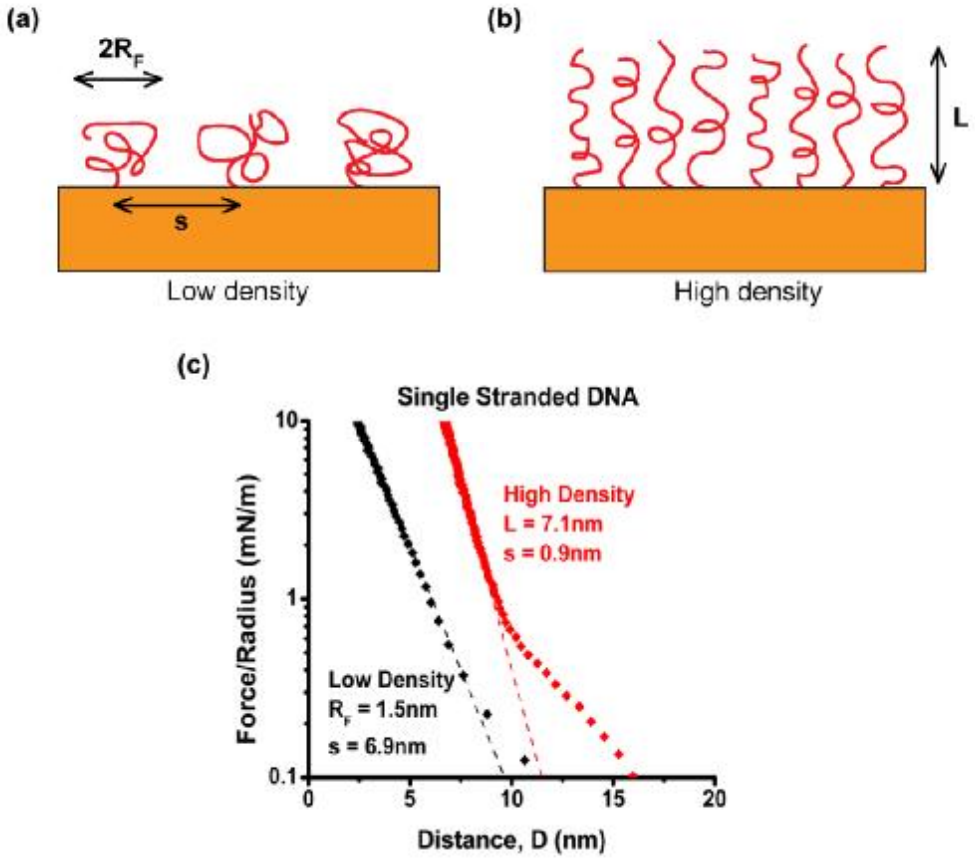

Figure 5-4. Increasing the density σ, single-stranded DNA monolayer leads to a structural change of the DNA monolayer. (a) At a grafting density of σ = 0.005 chain/nm^2, the repulsion force starts at10 nm, and shifts out to 15 nm after hybridization. (b) The repulsion force starts at a further distance ~ 15nm, and only shifts out by 2 nm after hybridization for a single-stranded DNA monolayer with a grafting density of σ = 0.1 chain/nm^2.

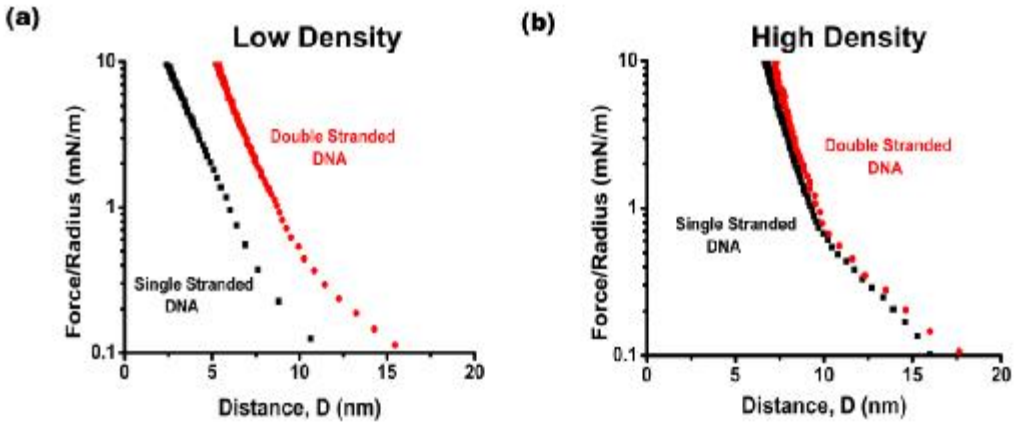

Figure 5-5. (a) In the low density condition, σ = 0.01 chain/nm^2, after single stranded DNA has been hybridized, the force curve shifts out to 15 nm after hybridization. (b) In the high density condition, the hybridization only make the force cuver shifts out by 1~2 nm with a grafting density of σ = 0.1 chain/nm^2.

The grafting density of the single-stranded DNA monolayer also affects mechanical response of double-stranded DNA monolayer after hybridization. For a DNA monolayer of σ = ~ 0.01 chain/nm^2,a significant increase in repulsion force was measured in the SFA force profile after hybridization, where as no big change was observed in force distance profiles of the high density DNA monolayer measured before and after hybridization. A denser single-stranded DNA film could lead to stronger steric hinder effect, which could affect the equilibrium and kinetics of the hybridization process. This hindering effect has also been observed in previous E-DNA sensor studies.

The structure of surface tethered short DNA oligomers attracts a great deal of interests in recent years for DNA microarray related technological applications.[2, 9,

28] Our SFA results demonstrate that the configuration of sparely grafted single-stranded DNA exhibit a mushroom like structure, which is similar to the structure of surface tethered polyelectrolyte under similar conditions. After hybridization, the double-stranded DNA transit into a rod like structure, resulting in a stiffer monolayer and stronger repulsion. The configuration of the surface tethered short DNA oligomers is determined by the hybridization state of the DNA monolayer, the concentration of complementary DNA in solution, and the grafting density. We show that the SFA can be a very useful technique to reveal the structure of surface tethered DNA, providing useful guidelines for the design of DNA sensors and sensor arrays.

5.4 Experiment and method

Reagents. PBS (Sigma Aldrich), NaCl (Sigma Aldrich), 6-Mercapto-1-hexanol (Sigma Aldrich), deionized (DI) water (MilliporeA), tris(2-carboxyethyl)phosphine hydrochloride (Molecular Probes, Carlsbad, CA)The probe and target DNA sequences (Biosearch Technologies – Novato, CA) are

Probe: 5' - HS-$(CH_2)_6$- TTATTGATCGGCGTTTTAAAGAAG - 3'

Target: 3' - CTAGCCGCAAAT - 5'

Probe: 5' - HS-$(CH_2)_6$–ACCCTGAAGTTCATCTGCACCACCG - 3'

Target: 3' - TGGGACTTCAAGTAGACGTGGTGGC - 5'

Gold Surface Preparation. Atomically smooth gold surfaces were prepared usinga mica templating technique. First, a gold layer (45 nm thick) was depositedon a freshly cleaved mica sheet. The mica sheet then was glued onto a cylindricalglass disk using an UV-curable glue with the gold layer facing down tothe UV glue. Then the glue was fully cured by exposing to UV light for 3 hr. Themica sheet was peeled off in ethanol to reveal the atomically smooth goldsurface that is predominantly single-crystalline goldwith a unit cell dimension of <111>.

DNA Grafting. DNA grafted surfaces were prepared using a well-established procedure. In brief, prior to sensor fabrication, The linear probe DNAs, used as delivered, were reduced for 1 hr at room temperature in the dark in 10 mMtris(2-carboxyethyl)phosphine hydrochloride and then diluted to a final concentration of 1.0 μM in phosphate-buffered saline (PBS)/NaCl buffer (The NaCl concentration depend on experiment requirement, this will be noticed in results

discussion). The gold surfaces were incubated in this solutionat room temperature in the dark, rinsed with deionized (DI) water, and then incubated in 3 mM 6-mercapto-1-hexanol in DI water for 2hr. Following this, the surfaces were rinsed in DI water and stored in PBS/NaCl buffer until used.

Surface Force Measurement. The normal forces of a gold surface grafted by DNA oligomers and a bare mica surface was measured using an SFA 2000 (manufactured by SurForce LLC, Santa Barbara, CA) with a reported geometry.[24, 25]Briefly, a DNA grafted gold surface was mounted in the SFA chamber facing a bare mica surface. The gap between two surfaces was filled with buffer solution. The force between two surfaces was measured as a function of the distance between two surfaces (Figure 1a).The distance between the surfaces *D* is measured with an optical technique based on multiple beam interference fringes (fringes of equal chromatic order, FECO) where *D* is determined with a resolution of 1Å from measurements of the wavelength of the FECO fringes in a spectrometer. The two surfaces were brought into contact or separated by a motor with a speed of 2-3 nm/s. After the measurements with single-stranded DNA, the sample surface was take out of the SFA chamber and dipped in target DNA solution at certain concentration for 2 hr. After the DNA hybridization, the sample was rinsed by PBS/NaCl buffer, and mounted back to SFA chamber for one double-stranded DNA measurement. Due to differences in the radius of the surfaces *R* from the gluing process it is customary to normalize the force *F* by *R* when comparing SFA measurements. The normalized force *F/R* between the two cylindrical SFA surfaces is directly proportional to the

energy between two flat surfaces by the Derjaguin approximation.

5.4 Acknowledgment

This work was supported by the NIH (R01AI107936) (Kevin W. Plaxco)

5.5 Reference

1. Kang, D., et al., *Re-engineering Electrochemical Biosensors To Narrow or Extend Their Useful Dynamic Range.* Angewandte Chemie-International Edition, 2012. **51**(27): p. 6717-6721.
2. Yu, J., et al., *Microfluidics-Based Single-Cell Functional Proteomics for Fundamental and Applied Biomedical Applications.* Annual Review of Analytical Chemistry, Vol 7, 2014. **7**: p. 275-295.
3. Xue, M., et al., *Chemical Methods for the Simultaneous Quantitation of Metabolites and Proteins from Single Cells.* Journal of the American Chemical Society, 2015. **137**(12): p. 4066-4069.
4. Drummond, T.G., M.G. Hill, and J.K. Barton, *Electrochemical DNA sensors.* Nature Biotechnology, 2003. **21**(10): p. 1192-1199.
5. Hsieh, K., et al., *Integrated Electrochemical Microsystems for Genetic Detection of Pathogens at the Point of Care.* Accounts of Chemical Research, 2015. **48**(4): p. 911-920.
6. White, R.J., et al., *Wash-free, Electrochemical Platform for the Quantitative, Multiplexed Detection of Specific Antibodies.* Analytical Chemistry, 2012. **84**(2): p. 1098-1103.
7. Kelley, S.O., et al., *Advancing the speed, sensitivity and accuracy of biomolecular detection using multi-length-scale engineering.* Nature Nanotechnology, 2014. **9**(12): p. 969-980.
8. Lubin, A.A. and K.W. Plaxco, *Folding-Based Electrochemical Biosensors:*

The Case for Responsive Nucleic Acid Architectures. Accounts of Chemical Research, 2010. **43**(4): p. 496-505.

9. Halperin, A., A. Buhot, and E.B. Zhulina, *Brush effects on DNA chips: thermodynamics, kinetics, and design guidelines.* Biophysical Journal, 2005. **89**(2): p. 796-811.
10. Bracha, D., et al., *Entropy-driven collective interactions in DNA brushes on a biochip.* Proceedings of the National Academy of Sciences of the United States of America, 2013. **110**(12): p. 4534-4538.
11. Kegler, K., et al., *Polyelectrolyte-compression forces between spherical DNA brushes.* Physical Review Letters, 2008. **100**(11): p. 4.
12. Li, D.C., S. Banon, and S.L. Biswal, *Bending dynamics of DNA-linked colloidal particle chains.* Soft Matter, 2010. **6**(17): p. 4197-4204.
13. Cho, Y.K., et al., *A surface forces study of DNA hybridization.* Langmuir, 2001. **17**(25): p. 7732-7734.
14. Gong, P., G.M. Harbers, and D.W. Grainger, *Multi-technique comparison of immobilized and hybridized oligonucleotide surface density on commercial amine-reactive microarray slides.* Analytical Chemistry, 2006. **78**(7): p. 2342-2351.
15. Bosco, A., et al., *Hybridization in nanostructured DNA monolayers probed by AFM: theory versus experiment.* Nanoscale, 2012. **4**(5): p. 1734-1741.
16. Wang, K., et al., *Exploring the motional dynamics of end-grafted DNA oligonucleotides by in situ electrochemical atomic force microscopy.* Journal

of Physical Chemistry B, 2007. **111**(21): p. 6051-6058.

17. Husale, S., H.H.J. Persson, and O. Sahin, *DNA nanomechanics allows direct digital detection of complementary DNA and microRNA targets.* Nature, 2009. **462**(7276): p. 1075-U138.

18. Kimura-Suda, H., et al., *Base-dependent competitive adsorption of single-stranded DNA on gold.* Journal of the American Chemical Society, 2003. **125**(30): p. 9014-9015.

19. Petrovykh, D.Y., et al., *Nucleobase orientation and ordering in films of single-stranded DNA on gold.* Journal of the American Chemical Society, 2006. **128**(1): p. 2-3.

20. He, L., et al., *Colloidal Au-enhanced surface plasmon resonance for ultrasensitive detection of DNA hybridization.* Journal of the American Chemical Society, 2000. **122**(38): p. 9071-9077.

21. Kaiser, W. and U. Rant, *Conformations of End-Tethered DNA Molecules on Gold Surfaces: Influences of Applied Electric Potential, Electrolyte Screening, and Temperature.* Journal of the American Chemical Society, 2010. **132**(23): p. 7935-7945.

22. Gong, P. and R. Levicky, *DNA surface hybridization regimes.* Proceedings of the National Academy of Sciences of the United States of America, 2008. **105**(14): p. 5301-5306.

23. Anne, A. and C. Demaille, *Dynamics of electron transport by elastic bending of short DNA duplexes. Experimental study and quantitative*

modeling of the cyclic voltammetric behavior of 3 '-ferrocenyl DNA end-grafted on gold. Journal of the American Chemical Society, 2006. **128**(2): p. 542-557.

24. Israelachvili, J., et al., *Recent advances in the surface forces apparatus (SFA) technique.* Reports on Progress in Physics, 2010. **73**(3): p. 036601.

25. Yu, J., et al., *Adaptive hydrophobic and hydrophilic interactions of mussel foot proteins with organic thin films.* Proceedings of the National Academy of Sciences of the United States of America, 2013. **110**(39): p. 15680-15685.

26. Anderson, T.H., et al., *Direct Measurement of Double-Layer, van der Waals, and Polymer Depletion Attraction Forces between Supported Cationic Bilayers.* Langmuir, 2010. **26**(18): p. 14458-14465.

27. Zuker, M., *Mfold web server for nucleic acid folding and hybridization prediction.* Nucleic Acids Research, 2003. **31**(13): p. 3406-3415.

28. Leunissen, M.E., et al., *Quantitative Study of the Association Thermodynamics and Kinetics of DNA-Coated Particles for Different Functionalization Schemes.* Journal of the American Chemical Society, 2010. **132**(6): p. 1903-1913.